TECHNICAL RESEARCH REPORT

A *2D* Nondestructive Inspection Method to Detect a Through Crack by Electrostatic Boundary Measurements

by C. Berenstein, D-C. Chang and E. Wang

T.R. 96-1

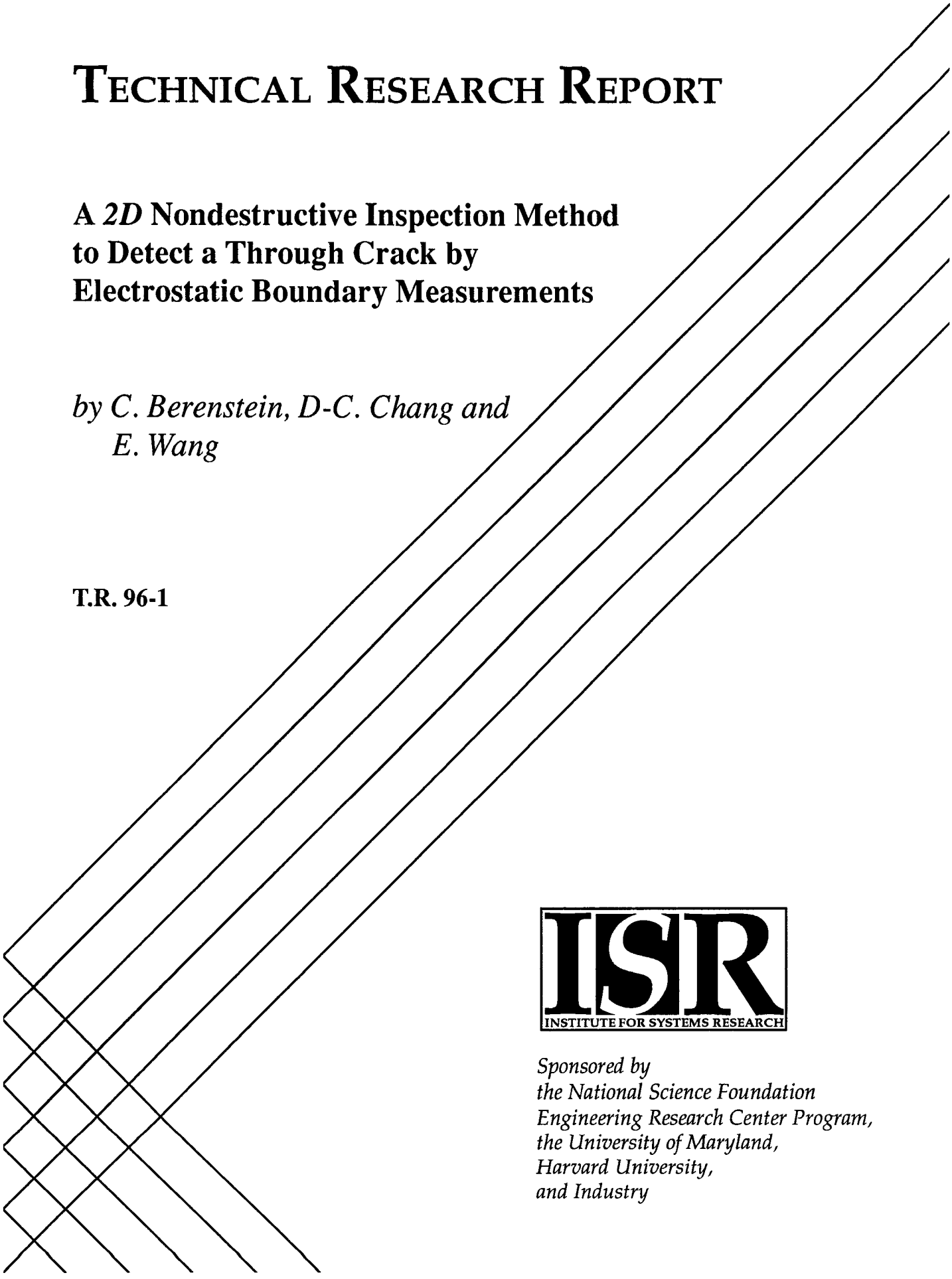

Sponsored by
the National Science Foundation
Engineering Research Center Program,
the University of Maryland,
Harvard University,
and Industry

A $2D$ NONDESTRUCTIVE INSPECTION METHOD TO DETECT A THROUGH CRACK BY ELECTROSTATIC BOUNDARY MEASUREMENTS

CARLOS BERENSTEIN, DER-CHEN CHANG AND EMEI WANG

University of Maryland, College park

0. Introduction. In the paper [FV], defect determination for electrically conductible specimens by using electrostatic boundary measurement was first time modeled as an inverse boundary value problem. Some studies about interior cracks have been done numerically or analytically [A, ABV, BV1, BV2, KS, KSV, SV]. It is our intent in this paper to study the detectability of a surface crack at its early stage of growth by means of the electrostatic potential field method. Uniqueness results of determining surface cracks have been established in [EIN]. In [EIN, EH], some computational methods are also developed for polygonal and/or doubly connected domains. We explore the case of simple geometry, namely, a circular cylinder which has a crack plane somewhere penetrating the side wall. Assume the plate has a constant conductivity (WLOG, say, equal to 1), and the crack plane is all the way through the thickness of the cylinder in the z-direction. From both practical and technical point of view, there are a couple of reasons to tackle this type of through crack (meaning, the crack with through-thickness in one dimension of the probed specimen).

(1) Lab experiments indicate the effect of potential field-flaw interaction with smooth crack surface is less prominent than that with rough crack surface [C]. In other words, a defect with rough crack surface should be detectable by means of a field method if the case with smooth crack surface has certain detectability.
(2) Due to the cylindrical homogeneity of the probed model in the z-direction, and the negligible thickness, the model can be treated by a $2D$ method.
(3) It is more difficult to probe a defect at its early stage of growth. Since a smooth crack can be regarded as a C^2 curve in many $2D$ models, the crack can be approximately treated as a line segment when the flaw size is small.

So. we will consider a planar disk with a radial slit penetrating the circumference. Let $\Omega \subset \mathbb{R}^2$ represent the disk and denote by $\partial\Omega$ the boundary of Ω. Let σ stand for the crack. Assume the crack is perfect insulating. Suppose one imposes a dipole Neumann condition on $\partial\Omega$. then the induced electrostatic potential field u satisfies

the following PDE :

$$
\begin{aligned}
&\Delta u = 0 && \text{in} \quad \Omega \setminus \sigma, \\
&\frac{\partial u}{\partial \nu} = 0 && \text{on} \quad \sigma, \\
&\frac{\partial u}{\partial \nu} = \delta_P - \delta_Q && \text{on} \quad \partial\Omega,
\end{aligned} \tag{0.1}
$$

where $\frac{\partial}{\partial \nu}$ denotes the outward normal derivative, P and Q stand for the locaitons of the dipole. In the context of physics, $\frac{\partial u}{\partial \nu}$ represents the current flux density. (Theoretically) We can generate the given Neumann boundary condition in (0.1) by setting two (point) current electrodes at P and Q and applying DC current to the boundary of the probed domain Let f represent the corresponding Dirichlet condition, i.e.,

$$
f = u\big|_{\partial\Omega}, \tag{0.2}
$$

and denote by $\frac{\partial}{\partial \tau}$ the tangential derivative along $\partial\Omega$. The solution to (0.1) is not unique (it is unique up to some constant). However, by taking $\frac{\partial f}{\partial \tau}$, this boundary measurement is unique. The physical meaning of $\frac{\partial f}{\partial \tau}$ will be the infinitesimal chage of the electrical potential in the direction along the boundary. The inverse problem pertaining to this model can be phrased in the following manner : " Given P, Q, and measuring $\frac{\partial f}{\partial \tau}$, how do we determine the location and the length of σ ? " It turns out with particular choice of P and Q, we can construct a strictly increasing function of s in terms of $\frac{\partial f}{\partial \tau}$ measured at two specific locations on $\partial\Omega$. An immediate application of this result is the capability to determine whether a surface crack exists in the domain by the boundary measurements $\frac{\partial f}{\partial \tau}$ at two different locaitons of specific choice. Based on this result, we formulate two convergent numerical algorithms : one for locating the crack and the other for determining the crack length. Our detection algorithms are in nature very much different from those implemented in [SV, BV]. In [SV, BV], the inspection algorithms rely on Newton's method to solve the implicit functionals of σ which are derived based on some weighted integrals of Dirichlet boundary measurements. The weight functions have to be carefully chosen in order to achieve nonsigularity of the Jacobians, and this is the most difficult part comprised in the construction of those computational algorithms. Our algorithms completely avoid Newton's method whose covergence and efficiency depend on the corresponding Jacobian. We trap the surface crack tip in a small neighborhood using a besection procedure. The idea of the length algorithm is to construct a decreasing sequence of estimates which converges to the actual crack length. The main results will be presented in section 1. We leave the analysis to section 2, section 3 and the Appendix. In section 4, Numerical simulation is performed. Specifically when the crakc length is small, we have detailed discussion regarding the stability and the effectiveness of the method.

1. Main Results. In this section, we present the major results. Since we impose some assumptions on the characteristics of the material defect (i.e., a linear surface crack with radial orientation), the only crack parameters remained to be determined are the location of the exterior crack tip and the crack length. In Theorem 1, we explicitly formualte an exact formula of the tangential derivative of the electrical voltage potential on $\partial\Omega$ in terms of the locations of P, Q, and the crack parameters.

Theorem 1. *Let Ω be the unit disk centered at the origin in $\mathbb{R}^2$. Assume a linear crack, σ, of length s initializes from $\partial\Omega$ and lies perpendicular to $\partial\Omega$. In complex plane, let $z_\sigma = e^{i\theta_\sigma}$ be the location of the exterior crack tip on $\partial\Omega$. The diameter on which σ is located divides $\partial\Omega$ into two half circles, say, $\partial\Omega^+$ and $\partial\Omega^-$. Suppose $0 < s < 2$. Similarly, let $P = e^{ip}$ and $Q = e^{iq}$ be two distinct points on $\partial\Omega$ away from σ. We denote by $u_{p,q,\sigma}$ a solution to (0.1), and let $f_{p,q,\sigma}$ represent the Dirichlet boundary measurement, i.e.,*

$$f_{p,q,\sigma} = u_{p,q,\sigma}\big|_{\partial\Omega}, \tag{1.1}$$

where the subscripts indicate both of the incurred electrical potential field and the boundary measurement depend on p, q, and σ. Define

$$f^1_{p,q,\sigma}(\theta) := \frac{1}{2\pi}\frac{[K_s(q-\theta_\sigma) - K_s(p-\theta_\sigma)]\tan\left(\frac{\theta-\theta_\sigma}{2}\right)\sec^2\left(\frac{\theta-\theta_\sigma}{2}\right)}{K_s(\theta-\theta_\sigma)[K_s(\theta-\theta_\sigma) - K_s(p-\theta_\sigma)][K_s(\theta-\theta_\sigma) - K_s(q-\theta_\sigma)]},$$

$$f^2_{p,q,\sigma}(\theta) := \frac{1}{2\pi}\frac{[K_s(p-\theta_\sigma) - K_s(q-\theta_\sigma)]\tan\left(\frac{\theta-\theta_\sigma}{2}\right)\sec^2\left(\frac{\theta-\theta_\sigma}{2}\right)}{K_s(\theta-\theta_\sigma)[K_s(\theta-\theta_\sigma) + K_s(p-\theta_\sigma)][K_s(\theta-\theta_\sigma) + K_s(q-\theta_\sigma)]},$$

$$f^3_{p,q,\sigma}(\theta) := -\frac{1}{2\pi}\frac{[K_s(p-\theta_\sigma) + K_s(q-\theta_\sigma)]\tan\left(\frac{\theta-\theta_\sigma}{2}\right)\sec^2\left(\frac{\theta-\theta_\sigma}{2}\right)}{K_s(\theta-\theta_\sigma)[K_s(\theta-\theta_\sigma) - K_s(p-\theta_\sigma)][K_s(\theta-\theta_\sigma) + K_s(q-\theta_\sigma)]},$$

and

$$f^4_{p,q,\sigma}(\theta) := \frac{1}{2\pi}\frac{[K_s(p-\theta_\sigma) + K_s(q-\theta_\sigma)]\tan\left(\frac{\theta-\theta_\sigma}{2}\right)\sec^2\left(\frac{\theta-\theta_\sigma}{2}\right)}{K_s(\theta-\theta_\sigma)[K_s(\theta-\theta_\sigma) + K_s(p-\theta_\sigma)][K_s(\theta-\theta_\sigma) - K_s(q-\theta_\sigma)]},$$

where

$$K_s(x) := \left[\left(\frac{s}{2-s}\right)^2 + \tan^2\left(\frac{x}{2}\right)\right]^{1/2}. \tag{1.2}$$

Then for $\theta \neq p + 2n\pi$, $\theta \neq q + 2n\pi$, and $\theta \neq \theta_\sigma + 2n\pi$ with $n \in \mathbb{Z}$, in polar coordinates,

(1.3)

$$\frac{\partial f_{p,q,\sigma}}{\partial\tau}(\theta) = \begin{cases} f^1_{p,q,\sigma}(\theta), & \text{when } P,\ Q, \text{ and } z \text{ are all on the same half circle,} \\ f^2_{p,q,\sigma}(\theta), & \text{when } P \text{ and } Q \text{ are on the same half circle, while } z \text{ is on the other half circle,} \\ f^3_{p,q,\sigma}(\theta), & \text{when } P \text{ and } z \text{ are on the same half circle, while } Q \text{ is on the other half circle,} \\ f^4_{p,q,\sigma}(\theta), & \text{when } Q \text{ and } z \text{ are on the same half circle, while } P \text{ is on the other half circle,} \end{cases}$$

where $z = e^{i\theta}$ is the location on $\partial\Omega$ where the boundary value $\frac{\partial f_{p,q,\sigma}}{\partial \tau}$ is measured, and whenever "the half circle" is mentioned, it always refers to $\partial\Omega^+$ or $\partial\Omega^-$.

To determine the location and the size of the crack through the knowledge of the boundary measurements (p, q, and $\frac{\partial f}{\partial \tau}$), we have to solve the nonlinear equations (1.3) for θ_σ (exterior crack tip) and s (crack length). One has to calculate the Jacobian of the system (1.3) if using Newton's method to directly solve (1.3) for (s,θ_σ) simultaneously. This involves choosing the optimal locations of P and Q – the choice of P and Q is optimal in the sense that the corresponding Jacobian of (1.3) is most nonsingular. Instead, we develop a convergent algorithm to independently trap the exterior crack tip in a "sufficiently" small neighborhood on $\partial\Omega$. After the surface crack tip is located, only s remaines to be solved in (1.3). Though we can solve the nonlinear equation (1.3) for s by means of Newton's mehtod, instead, we construct a completely different iteration procedure. This algorithm creates a sequencce of estimates which converges to the crack length.

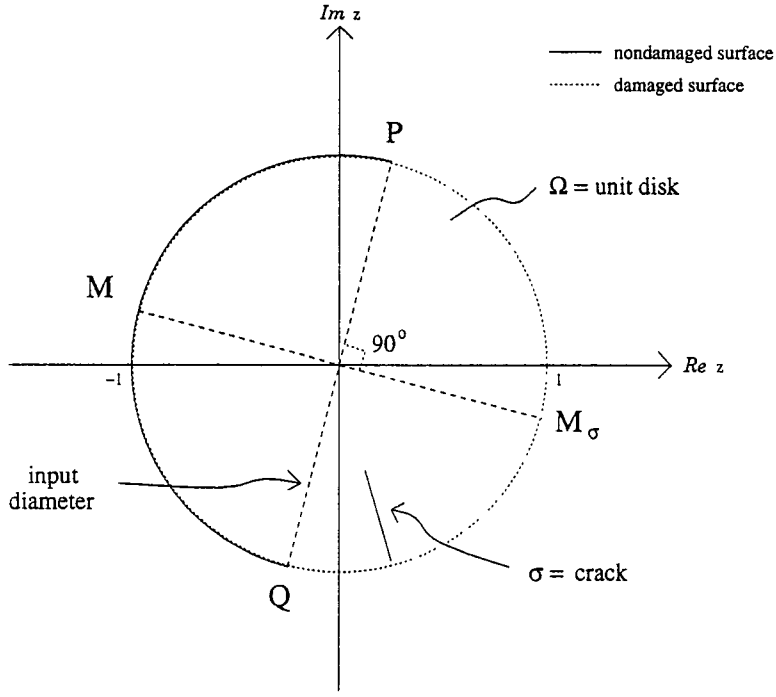

FIGURE 1

When a surface crack exists in the disk, two electrodes P and Q always divide the unit circle into two arcs : one represents the undamaged surface, and the other represents the damaged surface on which the exterior crack tip is located. Let M be the midpoint between P and Q on the undamaged surface. Let M_σ be the midpoint between P and Q on the damaged part and denote by M_0 for the case of an empty crack. When P and Q are located on the opposite ends of an arbitrary diameter of the unit disk (let us refer to this diameter as an "**input diameter**", Figure 1), then

Claim :

(1) $|\frac{\partial f_{p,q,\sigma}}{\partial \tau}(m)| = |\frac{\partial f_{p,q,\sigma}}{\partial \tau}(m_0)|$ *(the case where no crack exists).*

(2) $|\frac{\partial f_{p,q,\sigma}}{\partial \tau}(m)| > |\frac{\partial f_{p,q,\sigma}}{\partial \tau}(m_\sigma)|$ *(the case where a crack with length s exists).*

where $M = e^{im}$, $M_0 = e^{im_0}$, *and* $M_\sigma = e^{im_\sigma}$.

The above claim is the result of the following theorem :

Theorem 2. *Assume all the assumptions in Theorem 1 are satisfied. Suppose* $|p - q| = \pi$, *so that* q, m *and* m_σ *depend on* p. *Define*

$$\gamma_{p,\theta_\sigma}(s) := \left|\frac{\partial f_{p,q,\sigma}}{\partial \tau}(m)\right| \Big/ \left|\frac{\partial f_{p,q,\sigma}}{\partial \tau}(m_\sigma)\right|. \tag{1.4}$$

Then $\gamma_{p,\theta_\sigma}(s)$ *is a continuous, increasing function of* s *on [0,2) for each fixed pair of* $\{p, \theta_\sigma\}$, *such that* $p \neq \theta_\sigma + 2n\pi$, $n \in \mathbb{Z}$. *More precisely,*

$$\gamma_{p,\theta_\sigma}(s) = 1 + \eta_{p,\theta_\sigma}(s) \cdot s, \qquad 0 < s < 2, \tag{1.5}$$

where $\eta_{p,\theta_\sigma}(s) \geq 0$, *depends on* s *and the relative orientation of the "input diameter" with respect to the surface crack tip. Moreover, Assume* s_b *is any upper bound of* s *less than 2, i.e.,* $0 \leq s \leq s_b < 2$. *Let* $K_s(\theta)$ *be the same as in (1.2). Define*

$$A_{p,\theta_\sigma}(y) = |K_y(m_\sigma - \theta_\sigma) \cdot [K_y(m_\sigma - \theta_\sigma) - K_y(q - \theta_\sigma)]|, \tag{1.6}$$

$$B_{p,\theta_\sigma}(y) = \left|\frac{K_y(m_\sigma - \theta_\sigma) + K_y(p - \theta_\sigma)}{K_y(m - \theta_\sigma) + K_y(q - \theta_\sigma)}\right|, \tag{1.7}$$

$$C_{p,\theta_\sigma}(y) = \left|\frac{1}{K_y(m - \theta_\sigma)[K_y(m - \theta_\sigma) - K_y(p - \theta_\sigma)]}\right|, \tag{1.8}$$

and

$$D_{p,\theta_\sigma} = \left|\frac{\tan\left(\frac{m-\theta_\sigma}{2}\right)\sec^2\left(\frac{m-\theta_\sigma}{2}\right)}{\tan\left(\frac{m_\sigma-\theta_\sigma}{2}\right)\sec^2\left(\frac{m_\sigma-\theta_\sigma}{2}\right)}\right| = \frac{K_0(m - \theta_\sigma)[K_0^2(m - \theta_\sigma) + 1]}{K_0(m_\sigma - \theta_\sigma)[K_0^2(m_\sigma - \theta_\sigma) + 1]}. \tag{1.9}$$

For convenience, let's denote

$$\begin{cases} a = A_{p,\theta_\sigma}(0), \\ b = B_{p,\theta_\sigma}(0), \\ c = C_{p,\theta_\sigma}(0), \\ d = D_{p,\theta_\sigma}. \end{cases} \tag{1.10}$$

For fixed p, *define*

(1.11)

$$\begin{cases} \psi_1(\theta, x) = \frac{[K_x(q-\theta) - K_x(m_\sigma - \theta)]^2}{K_x(m_\sigma - \theta)K_x(q-\theta)}, \\ \psi_2(\theta, x, y) = \frac{K_y(m_\sigma - \theta) + K_y(p-\theta)}{K_y(m-\theta) + K_y(q-\theta)} \cdot \left[\frac{1}{K_x(m_\sigma - \theta)K_x(p-\theta)} - \frac{1}{K_x(m-\theta)K_x(q-\theta)}\right], \\ \psi_3(\theta, x) = \frac{1}{K_x^3(m-\theta)K_x(p-\theta)}, \end{cases}$$

and simply denote

$$\Psi_1 = \psi_1(\theta_\sigma, 0), \quad \Psi_2 = \psi_2(\theta_\sigma, 0, s_b), \quad \textit{and} \quad \Psi_3 = \psi_3(\theta_\sigma, 0). \tag{1.12}$$

Then for $0 < p - \theta_\sigma \leq \pi/2$,

$$\eta_{p,\theta_\sigma}(s) \leq \frac{s}{(2-s)^2} \cdot \alpha(p, \theta_\sigma, s_b), \tag{1.13}$$

where

$$\begin{aligned} \alpha(p, \theta_\sigma, s_b) =& \frac{2d}{2 - s_b} \cdot (bc\Psi_1 + ac\Psi_2 + ab\Psi_3) \\ &+ \frac{4s_b^2 d}{(2-s_b)^4} \cdot (c\Psi_1\Psi_2 + a\Psi_2\Psi_3 + b\Psi_1\Psi_3) \\ &+ \frac{8s_b^4 d}{(2-s_b)^7} \cdot \Psi_1\Psi_2\Psi_3. \end{aligned} \tag{1.14}$$

Let $\widehat{PQ}$ denote the curve which one traverses from P to Q counterclockwise along $\partial\Omega$ and PQ stand for the arc length of $\widehat{PQ}$. In the following algorithm, P_j and Q_j stand for the locations of the current electrodes to be imposed on $\partial\Omega$ at the jth step. For each j, let R_j (or R) denote the midpoint of $\widehat{P_jQ_j}$ (or $\widehat{PQ}$ respectively) , and N_j (or N) the midpoint of $\widehat{Q_jP_j}$ (or $\widehat{QP}$ respectively). Let an upper case letter represent a point, and the corresponding lower case letter denote the angular measurement of this point in polar coordinates (e.g., $P = e^{ip}$, $R_j = e^{ir_j}$, etc..). Assume $P_jQ_j = \pi$ (Figure 2, Figure 3).

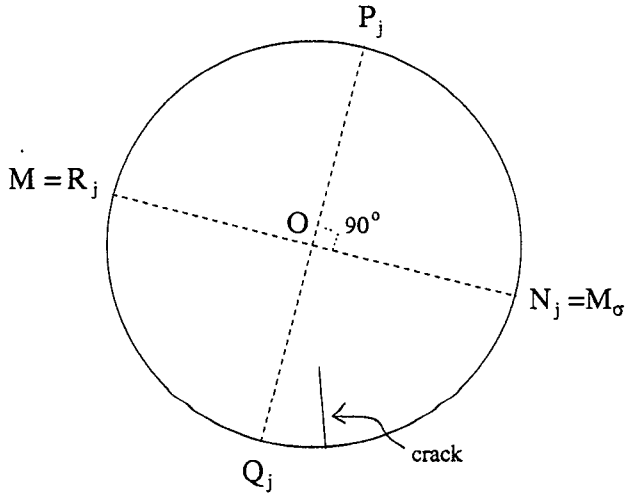

FIGURE 2

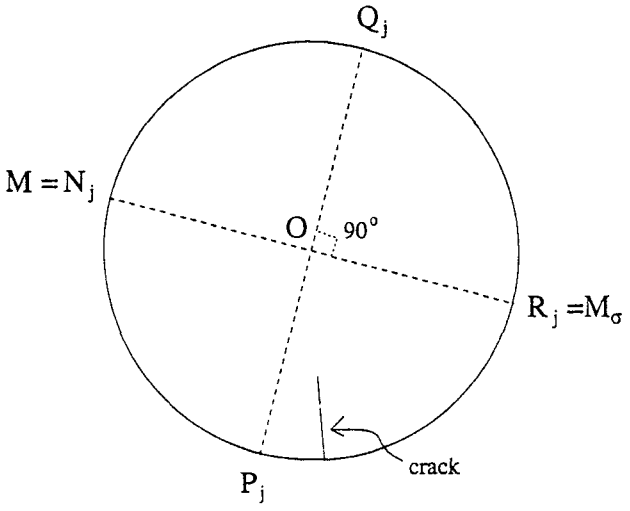

FIGURE 3

Consider the same PDEs as (0.1) at a set of different dipole locations :

$$
\begin{aligned}
&\Delta w_j = 0 && \text{in} \quad \Omega \setminus \sigma, \\
&\frac{\partial w_j}{\partial \eta} = 0 && \text{on} \quad \sigma, \\
&\frac{\partial w_j}{\partial \eta} = \delta_{P_j} - \delta_{Q_j} && \text{on} \quad \partial\Omega,
\end{aligned} \tag{1.15}
$$

and let

$$
f_{p_j,q_j,\sigma} = w_j\big|_{\partial\Omega}. \tag{1.16}
$$

The claim prior to Theorem 2 implies $|\frac{\partial f_{p_j,q_j,\sigma}}{\partial \tau}(r_j)| = |\frac{\partial f_{p_j,q_j,\sigma}}{\partial \tau}(n_j)|$ if there is no crack inside the disk. Otherwise, $|\frac{\partial f_{p_j,q_j,\sigma}}{\partial \tau}(r_j)| > |\frac{\partial f_{p_j,q_j,\sigma}}{\partial \tau}(n_j)|$ if there is a crack penetrating the boundary somewhere on $\overset{\frown}{Q_jP_j}$, and $|\frac{\partial f_{p_j,q_j,\sigma}}{\partial \tau}(r_j)| < |\frac{\partial f_{p_j,q_j,\sigma}}{\partial \tau}(n_j)|$ if the crack penetrates the boundary somewhere on $\overset{\frown}{P_jQ_j}$. Based on this result, we prove the following theorem of convergence. This theorem will serve as the guidline to construct an iterative procedure for locating a surface crack

Theorem 3 (A Convergent Algorithm To Locate The Edge Crack Tip). *Let z_σ denote the location of the edge crack tip. Assume all the assumptions in Theorem 1 are satisfied when applied to the PDE (1.11) for each j. P_0 and Q_0 are given and $|p_0 - q_0| = \pi$. For $j = 0, 1, 2, ...$, P_j and Q_j are determined in the following way:*

(1) *If $|\frac{\partial f_{p_j,q_j,\sigma}}{\partial \tau}(r_j)| > |\frac{\partial f_{p_j,q_j,\sigma}}{\partial \tau}(n_j)|$, then rotate P_j and Q_j counterclockwise along $\partial\Omega$ through an angle of $\frac{\pi}{2^{j+1}}$ to obtain P_{j+1} and Q_{j+1} respectively.*

(2) *If $|\frac{\partial f_{p_j,q_j,\sigma}}{\partial \tau}(r_j)| < |\frac{\partial f_{p_j,q_j,\sigma}}{\partial \tau}(n_j)|$, then rotate P_j and Q_j clockwise along $\partial\Omega$ through an angle of $\frac{\pi}{2^{j+1}}$ to obtain P_{j+1} and Q_{j+1} respectively.*

Then

$$
Q_j \to z_\sigma, \qquad as \quad j \to \infty.
$$

Moreover,

$$\angle Q_j O z_\sigma \le \frac{\pi}{2^j}, \qquad \forall j = 0, 1, 2, ...,$$

where O is the center of the unit disk and $\angle WYZ$ stands for the acute angle measurement of an angle $\angle WYZ$.

Last, we would like to present the result regarding length determination. For fixed p, define

$$\begin{cases} \phi_1(\theta,x,y) = & \frac{2y}{(2-y)^3}\cdot\frac{[K_x(q-\theta)-K_x(m_\sigma-\theta)]^2}{K_x(m_\sigma-\theta)K_x(q-\theta)}, \\ \phi_2(\theta,x,y) = & \frac{2y}{(2-y)^3}\cdot\frac{K_y(m_\sigma-\theta)+K_y(p-\theta)}{K_y(m-\theta)+K_y(q-\theta)}\cdot \\ & \left[\frac{1}{K_x(m_\sigma-\theta)K_x(p-\theta)}-\frac{1}{K_x(m-\theta)K_x(q-\theta)}\right], \\ \phi_3(\theta,x,y) = & \frac{2y}{(2-y)^3}\cdot\frac{1}{K_x^3(m-\theta)K_x(p-\theta)}. \end{cases} \tag{1.17}$$

Let

$$\begin{aligned} \beta(p,\theta,x,y) =& D_{p,\theta}\big[B_{p,\theta}(y)C_{p,\theta}(y)\phi_1(\theta,x,y) + A_{p,\theta}(y)C_{p,\theta}(y)\phi_2(\theta,x,y)+ \\ & A_{p,\theta}(y)B_{p,\theta}(y)\phi_3(\theta,x,y) + \phi_1(\theta,x,y)\phi_2(\theta,x,y)\phi_3(\theta,x,y)\big]. \end{aligned} \tag{1.18}$$

Given σ and p, define

$$\begin{aligned} \omega^1_{\sigma,p}(\theta,x,y) = \max\Bigg\{ & \min\left\{ y - \frac{\gamma_{p,\theta}(y)-\gamma_{p,\theta_\sigma}(s)}{\beta(p,\theta,x,y)}, y - \frac{\gamma_{p,\theta}(y)-\gamma_{p,\theta_\sigma}(s)}{\beta(p,\theta,\tilde{x},y)} \right\}, \\ & \min\left\{ y-1, y - \sqrt[3]{\frac{\gamma_{p,\theta}(y)-\gamma_{p,\theta_\sigma}(s)}{\beta(p,\theta,x,y)}} \right\} \Bigg\}, \end{aligned} \tag{1.19}$$

and

$$\omega^2_p(\theta,x,y) = \max\left\{ y - \frac{A_{p,\theta}(y)}{\phi_1(\theta,x,y)}, y - \frac{B_{p,\theta}(y)}{\phi_2(\theta,x,y)}, y - \frac{C_{p,\theta}(y)}{\phi_3(\theta,x,y)} \right\}, \tag{1.20}$$

where $\tilde{x} = \max(x, y-1)$. $\gamma_{p,\theta_\sigma}(\cdot)$ and $\alpha(\cdot,\cdot,\cdot)$ have been defined in Theorem 2. We construct two iteration functions as follows:

$$\lambda_{\sigma,p}(\theta,y) = 2\sqrt{\frac{\gamma_{p,\theta_\sigma}(s)-1}{\alpha(p,\theta,y)}} \Bigg/ \left(1+\sqrt{\frac{\gamma_{p,\theta_\sigma}(s)-1}{\alpha(p,\theta,y)}}\right), \tag{1.21}$$

and

$$\omega_{\sigma,p}(\theta,x,y) = \begin{cases} \omega^1_p(\theta,x,y), & \text{if } \gamma_{p,\theta_\sigma}(s) \ge \gamma_{p,\theta}\big(\omega^2_p(\theta,x,y)\big) \\ & \text{or } \omega^2_p(\theta,x,y) < 0\ , \\ \omega^2_p(\theta,x,y), & \text{otherwise.} \end{cases} \tag{1.22}$$

The subscripts of $\omega^1_{\sigma,p}$, ω^2_p, $\lambda_{\sigma,p}$ and $\omega_{\sigma,p}$ indicate these functions depend on the locations of the current electrodes and/or the geometric characteristics of the crack. We prove the following theorem in order to propose an effective procedure to estimate the crack length.

Theorem 4 (A Convergent Iterative Scheme to estimate the crack length). *Suppose p is chosen so that $0 < p - \theta_\sigma < \pi/2$. Assume $0 < s < s_b$ for some upper bound $s_b < 2$. Let*

$$\begin{cases} s_0 = s_b, \\ t_0 = \lambda_{\sigma,p}(\theta_\sigma, s_0) = \lambda_{\sigma,p}(\theta_\sigma, s_b), \\ \textit{and for } j = 0,1,2,3,\ldots, \\ s_{j+1} = \omega_{\sigma,p}(\theta_\sigma, t_j, s_j), \\ t_{j+1} = \lambda_{\sigma,p}(\theta_\sigma, s_{j+1}). \end{cases} \tag{1.23}$$

Then

$$0 < t_0 < t_1 < t_2 < \cdots < s < \cdots < s_2 < s_1 < s_0 = s_b. \tag{1.24}$$

and,

$$s_j \to s \quad as \quad j \to \infty. \tag{1.25}$$

Remark. Using similar arguments, it is still possible to construct and prove a convergent algorithm if the condition $0 < p - \theta_\sigma < \pi/2$ failes. We consider $0 < p - \theta_\sigma < \pi/2$ simply for the following reason : Due to the circular symmetry of the geometry, all the possibile degrees of sensitivity of the method corresponding to different locations of the current electrodes P and Q can be discussed within this range. Regarding the issue of sensitivity, we make observations and have some discussion in Section 4.

In Section 2, we present the proofs of Theorem 1 and Theorem 2. The proofs of Theorem 3 and Theorem 4 are arranged in Section 3.

2. Proof of Theorem 1. First of all, we need explictly solve the direct problem

$$
\begin{aligned}
&\Delta u = 0 && \text{in} \quad \Omega \setminus \sigma, \\
&\frac{\partial u}{\partial \nu} = 0 && \text{on} \quad \sigma, \\
&\frac{\partial u}{\partial \nu} = \delta_P - \delta_Q && \text{on} \quad \partial\Omega.
\end{aligned} \tag{2.1}
$$

Consider two delta families, $\{g_n^P\}_{n\in\mathbb{N}}$ and $\{g_n^Q\}_{n\in\mathbb{N}} \subset \mathrm{C}(\partial\Omega)$, whose compact supports are away from σ, such that

$$
\begin{aligned}
&\lim_{n\to\infty} g_n^P(x) = \delta_P(x), \\
&\lim_{n\to\infty} g_n^Q(x) = \delta_Q(x)
\end{aligned} \tag{2.2}
$$

in the sense of distribution, and

$$
\int_{\partial\Omega} g_n^P ds = \int_{\partial\Omega} g_n^Q ds.
$$

Let u_n satisfy the boundary value problem:

$$
\begin{aligned}
&\Delta u_n = 0 && \text{in} \quad \Omega \setminus \sigma, \\
&\frac{\partial u_n}{\partial \nu} = 0 && \text{on} \quad \sigma, \\
&\frac{\partial u_n}{\partial \nu} = g_n^P - g_n^Q && \text{on} \quad \partial\Omega.
\end{aligned} \tag{2.3}
$$

The solution to (2.3) is unique up to a constant. We normalize the solution by imposing the condition that $\int_{\partial\Omega} u_n = 0$. It's been understood that

$$
u_n \to u \quad \text{as} \quad j \to \infty \quad \text{in the sense of distribution.}
$$

In particular,

$$
\lim_{n\to\infty} u_n(z) = u(z), \qquad \forall z \in \Omega \setminus \sigma. \tag{2.4}
$$

Let h_σ be a one-to-one analytic transform that maps the connected domain $\Omega \setminus \sigma$ onto the unit disk Ω. Let $G(\cdot,\cdot)$ represent the Green's function for the Neumann Problem in Ω, and $G_\sigma(\cdot,\cdot)$ represent the Green's function for the Neumann Problem in $\Omega \setminus \sigma$. The Green's functions corresponding to the Laplace equation are conformally invariant, so

$$
G_\sigma(y,z) = G\big(h_\sigma(y), h_\sigma(z)\big), \quad \forall z \in \Omega \setminus \sigma.
$$

Therefore the solution to (2.3) is given by

$$
u_n(z) = \int_{\partial\Omega} \big(g_n^P(y) - g_n^Q(y)\big) G\big(h_\sigma(y), h_\sigma(z)\big) dy, \qquad z \in \Omega \setminus \sigma, \tag{2.5}
$$

since the Neumann boundary condition vanishes on σ which is regarded as part of $\partial(\Omega \setminus \sigma)$. Passing limits on both sides of (2.5) as $n \to \infty$, and applying (2.2) and (2.4), we have

$$u(z) = G\big(h_\sigma(P), h_\sigma(z)\big) - G\big(h_\sigma(Q), h_\sigma(z)\big), \qquad z \in \Omega \setminus \sigma. \tag{2.6}$$

In polar coordinates, the Green's function G reads

$$G(\rho, \phi, r, \theta) = -\frac{1}{4\pi} \log\big(r^2 + \rho^2 - 2r\rho\cos(\theta - \phi)\big)\big(1 + \rho^2 r^2 - 2r\rho\cos(\theta - \phi)\big). \tag{2.7}$$

We then apply (2.7) to (2.6) for $z = re^{i\theta}$. In polar coordinates, (2.6) reads

$$\begin{aligned}
u(r,\theta) =& G\big(|h_\sigma(P)|, \arg h_\sigma(P), |h_\sigma(re^{i\theta})|, \arg h_\sigma(re^{i\theta})\big) \\
& - G\big(|h_\sigma(Q)|, \arg h_\sigma(Q), |h_\sigma(re^{i\theta})|, \arg h_\sigma(re^{i\theta})\big), \\
=& -\frac{1}{4\pi} \log \Big[|h_\sigma(re^{i\theta})|^2 + |h_\sigma(P)|^2 - 2 \cdot h_\sigma(re^{i\theta})| \cdot |h_\sigma(P)| \cdot \\
& \cos\big(\arg h_\sigma(re^{i\theta}) - \arg h_\sigma(P)\big)\Big] \cdot \Big[1 + h_\sigma(P)|^2 \cdot |h_\sigma(re^{i\theta})|^2 \\
& - 2 \cdot |h_\sigma(re^{i\theta})| \cdot |h_\sigma(P)| \cdot \cos\big(\arg h_\sigma(re^{i\theta}) - \arg h_\sigma(P)\big)\Big] \\
& + \frac{1}{4\pi} \log \Big[|h_\sigma(re^{i\theta})|^2 + |h_\sigma(Q)|^2 - 2 \cdot h_\sigma(re^{i\theta})| \cdot |h_\sigma(Q)| \cdot \\
& \cos\big(\arg h_\sigma(re^{i\theta}) - \arg h_\sigma(Q)\big)\Big] \cdot \Big[1 + |h_\sigma(Q)|^2 \cdot |h_\sigma(re^{i\theta})|^2 \\
& - 2 \cdot |h_\sigma(re^{i\theta})| \cdot |h_\sigma(Q)| \cdot \cos\big(\arg h_\sigma(re^{i\theta}) - \arg h_\sigma(Q)\big)\Big], \\
& 0 \le r < 1, \quad \theta \ne \theta_\sigma.
\end{aligned} \tag{2.8}$$

In Appendix A, we explicitly construct h_σ for the case where $\theta_\sigma = 0$. The notations Ω^+, Ω^-, $\partial\Omega^+$, $\partial\Omega^-$, σ^+, and σ^- will follow the definitions (A.2) in Appendix A. Since $\Omega \setminus \sigma$ is not a smooth doamin, some properties of h_σ have to be carefully considered while carrying out the calcuations in order to solve the boundary value problem. Regarding this point, we have detailed discussion in Appendix A. Now, we claim that

$$h_\sigma(e^{i\theta}) = \begin{cases} \frac{1-K_s^2(\theta)}{1+K_s^2(\theta)} + \frac{2K_s(\theta)}{1+K_s^2(\theta)} i, & \text{if } \ 0 < \theta < \pi, \\ \frac{1-K_s^2(\theta)}{1+K_s^2(\theta)} - \frac{2K_s(\theta)}{1+K_s^2(\theta)} i, & \text{if } \ \pi < \theta < 2\pi, \\ -1, & \text{if } \ \theta = \pi, \end{cases} \tag{2.9}$$

where $K_s(\theta) := \left[\left(\frac{s}{2-s}\right)^2 + \tan^2\left(\frac{\pi}{2}\right)\right]^{1/2}$.

Given $z = e^{i\theta} \in \partial\Omega$, consider a sequence of points, $\{z_n = r_n e^{i\theta_n}\}_{n=1}^{\infty} \subset \Omega$, such that $z_n \to z$, as $n \to \infty$. That is, $r_n \to 1^-$, and $\theta_n \to \theta$ as $n \to \infty$. Then

(2.10)
$$\left(\frac{s}{2-s}\right)^2 - \left(\frac{z_n - 1}{z_n + 1}\right)^2 = \left(\frac{s}{2-s}\right)^2 - \frac{(r_n^2-1)^2 - 4r_n^2 \sin^2\theta_n}{\left[(r_n^2+1) + 2r_n\cos\theta_n\right]^2} - \frac{4r_n(r_n^2-1)\sin\theta_n}{\left[(r_n^2+1) + 2r_n\cos\theta_n\right]^2} i.$$

Let

(2.11)
$$w_n := \left(\frac{s}{2-s}\right)^2 - \left(\frac{z_n - 1}{z_n + 1}\right)^2 = \xi_n e^{i\psi_n}.$$

To keep analyticity of h_σ in the interior of the mapping domain $\Omega \setminus \sigma$, we must consider the branch $0 < \psi_n < 2\pi$, so that $w_n^{1/2} = \sqrt{\xi_n} e^{i\psi_n/2}$ (see Appendix A). Suppose $z \in \partial\Omega^+$, then the sequence is chosen to approach z from the interior of Ω^+. That is, $z_n \in \Omega^+$, $\forall n$. Thus, $\sin\theta_n > 0$ and $0 \le r_n < 1$. From (2.10) adn (2.11), we observe that $\mathrm{Im}(w_n) > 0$. This implies $0 < \psi_n < \pi$. Hence $0 < \psi_n/2 < \pi/2$. Moreover,

$$\begin{aligned}\lim_{n\to\infty} \mathrm{Re}(w_n) &= \lim_{n\to\infty} \left\{ \left(\frac{s}{2-s}\right)^2 - \frac{(r_n^2-1)^2 - 4r_n^2\sin^2\theta_n}{\left[(r_n^2+1) + 2r_n\cos\theta_n\right]^2} \right\} \\ &= \left(\frac{s}{2-s}\right)^2 + \frac{4\sin^2\theta}{(2+2\cos\theta)^2} \\ &= \left(\frac{s}{2-s}\right)^2 + \tan^2\frac{\theta}{2} \quad ,\end{aligned}$$

and

$$\lim_{n\to\infty} \mathrm{Im}(w_n) = \lim_{n\to\infty} \frac{-4r_n(r_n^2-1)\sin\theta_n}{\left[(r_n^2+1) + 2r_n\cos\theta_n\right]^2} = 0$$

Therefore, we obtain

$$\begin{aligned}\lim_{n\to\infty} \tan\frac{\psi_n}{2} &= \lim_{n\to\infty} \frac{\sin\psi_n}{1+\cos\psi_n} = \lim_{n\to\infty} \frac{\xi_n \sin\psi_n}{\xi_n + \xi_n\cos\psi_n} \\ &= \lim_{n\to\infty} \frac{\mathrm{Im}(w_n)}{\xi_n + \mathrm{Re}(w_n)} = \lim_{n\to\infty} \frac{\mathrm{Im}(w_n)}{(\mathrm{Re}w_n)^2 + (\mathrm{Im}w_n)^2 + \mathrm{Re}w_n} \\ &= 0.\end{aligned}$$

It immediately follows that $\frac{\psi_n}{2} \to 0$ since $0 < \psi_n/2 < \pi/2$, $\forall n$. So

(2.12)
$$\begin{aligned}\lim_{n\to\infty} w_n^{1/2} &= \lim_{n\to\infty} \sqrt{\xi_n} e^{i\psi_n/2} = \lim_{n\to\infty} \sqrt{(\mathrm{Re}w_n)^2 + (\mathrm{Im}w_n)^2} \\ &= \left[\left(\frac{s}{2-s}\right)^2 + \tan^2\frac{\theta}{2}\right]^{1/2}.\end{aligned}$$

Using the definition (A.3) in Appendix A and applying (2.12), we obtain

$$h_\sigma(e^{i\theta}) = \lim_{\Omega^+ \ni z_n \to z = e^{i\theta}} \frac{i - \left(\left(\frac{s}{2-s} \right)^2 - \left(\frac{z_n - 1}{z_n + 1} \right)^2 \right)^{1/2}}{i + \left(\left(\frac{s}{2-s} \right)^2 - \left(\frac{z_n - 1}{z_n + 1} \right)^2 \right)^{1/2}}$$

$$= \lim_{n \to \infty} \frac{i - w_n^{1/2}}{i + w_n^{1/2}} = \frac{i - \left(\left(\frac{s}{2-s} \right)^2 + \tan^2 \frac{\theta}{2} \right)^{1/2}}{i + \left(\left(\frac{s}{2-s} \right)^2 + \tan^2 \frac{\theta}{2} \right)^{1/2}}$$

$$= \frac{1 - K_s^2(\theta)}{1 + K_s^2(\theta)} + \frac{2K_s(\theta)}{1 + K_s^2(\theta)} i$$

for $0 < \theta < \pi$, as claimed in (2.9). Using similar argument, we assert that if $z \in \partial\Omega^-$, then $\psi_n \to \pi$ as $n \to \infty$. Analogous to (2.12), we have

$$\lim_{n \to \infty} w_n^{1/2} = \lim_{n \to \infty} -\sqrt{\xi}_n = -\left[\left(\frac{s}{2-s} \right)^2 + \tan^2 \frac{\theta}{2} \right]^{1/2}$$

and then,

$$h_\sigma(e^{i\theta}) = \lim_{\Omega^- \ni z_n \to z = e^{i\theta}} \frac{i - \left(\left(\frac{s}{2-s} \right)^2 - \left(\frac{z_n - 1}{z_n + 1} \right)^2 \right)^{1/2}}{i + \left(\left(\frac{s}{2-s} \right)^2 - \left(\frac{z_n - 1}{z_n + 1} \right)^2 \right)^{1/2}}$$

$$= \lim_{n \to \infty} \frac{i - w_n^{1/2}}{i + w_n^{1/2}} = \frac{i + \left(\left(\frac{s}{2-s} \right)^2 + \tan^2 \frac{\theta}{2} \right)^{1/2}}{i - \left(\left(\frac{s}{2-s} \right)^2 + \tan^2 \frac{\theta}{2} \right)^{1/2}}$$

$$= \frac{1 - K_s^2(\theta)}{1 + K_s^2(\theta)} - \frac{2K_s(\theta)}{1 + K_s^2(\theta)} i$$

for $\pi < \theta < 2\pi$. In particular, $w_n^{1/2} \to \infty$ when $\theta = \pi$ and the limit is approached from either Ω^+ or Ω^-. So

$$h_\sigma(e^{i\theta}) = \lim_{\Omega^+ \ni z_n \to z = e^{i\pi}} \frac{i - \left(\left(\frac{s}{2-s} \right)^2 - \left(\frac{z_n - 1}{z_n + 1} \right)^2 \right)^{1/2}}{i + \left(\left(\frac{s}{2-s} \right)^2 - \left(\frac{z_n - 1}{z_n + 1} \right)^2 \right)^{1/2}}$$

$$= \lim_{\Omega^- \ni z_n \to z = e^{i\pi}} \frac{i - \left(\left(\frac{s}{2-s} \right)^2 - \left(\frac{z_n - 1}{z_n + 1} \right)^2 \right)^{1/2}}{i + \left(\left(\frac{s}{2-s} \right)^2 - \left(\frac{z_n - 1}{z_n + 1} \right)^2 \right)^{1/2}}$$

$$= \lim_{n \to \infty} \frac{i - w_n^{1/2}}{i + w_n^{1/2}} = -1.$$

We have proved (2.9).

Now, we would like to formulate $f_{p,q,\sigma}$ from (2.8). There are four possibilities concerning the locations of P and Q. Case I : $0 < p, q < \pi$; Case II : $\pi < p, q < 2\pi$; Case III : $0 < p < \pi$, $\pi < q < 2\pi$; And Case IV : $\pi < p < 2\pi$, $0 < q < \pi$. We only discuss case I in the following paragraph. Calculations for the other cases are similar.

Case I : Suppose $0 < p, q < \pi$. Let $\arg h_\sigma(e^{i\theta}) = \phi$, $0 < \phi < 2\pi$. Since h_σ maps the boundary of $\Omega \setminus \sigma$ onto the unit circle, $|h_\sigma(e^{i\theta})| = 1$. We have

$$h_\sigma(e^{i\theta}) = e^{i\phi} = \cos\phi + i\sin\phi.$$

Comparing this expression with (2.9), it follows that

$$\cos\left(\arg h_\sigma(e^{i\theta})\right) = \frac{1 - K_s^2(\theta)}{1 + K_s^2(\theta)}, \qquad 0 < \theta < 2\pi, \tag{2.13}$$

and

$$\sin\left(\arg h_\sigma(e^{i\theta})\right) = \begin{cases} \frac{2K_s(\theta)}{1+K_s^2(\theta)}, & \text{if} \quad 0 < \theta < \pi, \\ -\frac{2K_s(\theta)}{1+K_s^2(\theta)}, & \text{if} \quad \pi < \theta < 2\pi. \end{cases} \tag{2.14}$$

Similarly, $|h_\sigma(P)| = |h_\sigma(Q)| = 1$,

(2.15)

$$\left\{ \begin{array}{l} \cos\left(\arg h_\sigma(e^{ip})\right) = \dfrac{1 - K_s^2(p)}{1 + K_s^2(p)} \\ \\ \sin\left(\arg h_\sigma(e^{ip})\right) = \dfrac{2K_s(p)}{1 + K_s^2(p)} \end{array} \right\}, \quad \text{and} \quad \left\{ \begin{array}{l} \cos\left(\arg h_\sigma(e^{iq})\right) = \dfrac{1 - K_s^2(q)}{1 + K_s^2(q)} \\ \\ \sin\left(\arg h_\sigma(e^{iq})\right) = \dfrac{2K_s(q)}{1 + K_s^2(q)} \end{array} \right\}.$$

Since $|h_\sigma(e^{i\theta})| = |h_\sigma(P)| = |h_\sigma(Q)| = 1$, Applying (2.8) to the definition (1,1), we obtain

$$\begin{aligned} f_{p,q,\sigma}(\theta) = \lim_{r\to 1^-} u(r,\theta) &= -\frac{1}{4\pi}\log[2 - 2\cos\left(\arg(h_\sigma(e^{i\theta}) - \arg(h_\sigma(P))\right)]\cdot \\ &\quad [2 - 2\cos\left(\arg(h_\sigma(e^{i\theta})) - \arg(h_\sigma(P))\right)] \\ &\quad + \frac{1}{4\pi}\log[2 - 2\cos\left(\arg(h_\sigma(e^{i\theta})) - \arg(h_\sigma(Q))\right)]\cdot \\ &\quad [2 - 2\cos\left(\arg(h_\sigma(e^{i\theta})) - \arg(h_\sigma(Q))\right)] \\ &= \frac{1}{2\pi}\log\left[\frac{1 - \cos\left(\arg(h_\sigma(e^{i\theta})) - \arg(h_\sigma(e^{iq}))\right)}{1 - \cos\left(\arg(h_\sigma(e^{i\theta})) - \arg(h_\sigma(e^{ip}))\right)}\right], \end{aligned} \tag{2.16}$$

whenever $\theta \neq 2n\pi$, $n \in \mathbb{Z}$. Based on the formula $\cos(\alpha-\beta) = \cos\alpha\cos\beta + \sin\alpha\sin\beta$ and unsing conditions (2.13)–(2.14), we have

$$\begin{aligned} &\cos\left(\arg h_\sigma(e^{i\theta}) - \arg h_\sigma(e^{iq})\right) \\ &= \frac{1 - K_s^2(\theta)}{1 + K_s^2(\theta)}\frac{1 - K_s^2(q)}{1 + K_s^2(q)} + \frac{2K_s(\theta)}{1 + K_s^2(\theta)}\frac{2K_s(q)}{1 + K_s^2(q)} \\ &= \frac{[1 + K_s(\theta)K_s(q)]^2 - [K_s(\theta) - K_s(q)]^2}{[1 + K_s^2(\theta)][1 + K_s^2(q)]}, \qquad 0 < \theta < \pi, \end{aligned} \tag{2.17}$$

and

$$\cos\left(\arg h_\sigma(e^{i\theta}) - \arg h_\sigma(e^{ip})\right) \tag{2.18}$$
$$= \frac{[1+K_s(\theta)K_s(p)]^2 - [K_s(\theta)-K_s(p)]^2}{[1+K_s^2(\theta)][1+K_s^2(p)]}, \qquad 0<\theta<\pi.$$

Now we substitute expressions (2.17)–(2.18) into the right-hand side of (2.15). Through some simplifications, we reduce (2.15) to the following equation:

$$f_{p,q,\sigma}(\theta) = \frac{1}{\pi}\log\left[\frac{K_s(\theta)-K_s(q)}{K_s(\theta)-K_s(p)}\right] + \frac{1}{2\pi}\log\left[\frac{1+K_s^2(p)}{1+K_s^2(q)}\right], \quad 0<\theta<\pi. \tag{2.19}$$

Note that on $\partial\Omega$,

$$\frac{\partial f_{p,q,\sigma}}{\partial\tau}(\theta) = \frac{\partial f_{p,q,\sigma}}{\partial\theta}(\theta).$$

So, when $0<p,q<\pi$ and $0<\theta<\pi$ (equivalently, $P,Q,z\in\partial\Omega^+$), we obtain

$$\frac{\partial f_{p,q,\theta}}{\partial\tau}(\theta) = f^1_{p,q,\sigma}(\theta)$$

by differentiating (2.19) on both sides with respect to θ.

In case $\pi<\theta<2\pi$, instead of (2.17) and (2.18), we have

$$\cos\left(\arg h_\sigma(e^{i\theta}) - \arg h_\sigma(e^{iq})\right)$$
$$= \frac{1-K_s^2(\theta)}{1+K_s^2(\theta)}\frac{1-K_s^2(q)}{1+K_s^2(q)} + \frac{-2K_s(\theta)}{1+K_s^2(\theta)}\frac{2K_s(q)}{1+K_s^2(q)}$$
$$= \frac{[1-K_s(\theta)K_s(q)]^2 - [K_s(\theta)+K_s(q)]^2}{[1+K_s^2(\theta)][1+K_s^2(q)]}, \qquad \pi<\theta<2\pi,$$

and

$$\cos\left(\arg h_\sigma(e^{i\theta}) - \arg h_\sigma(e^{ip})\right)$$
$$= \frac{[1-K_s(\theta)K_s(p)]^2 - [K_s(\theta)+K_s(p)]^2}{[1+K_s^2(\theta)][1+K_s^2(p)]}, \qquad \pi<\theta<2\pi.$$

Repeating the same course of computations as for the case $0<\theta<\pi$, we obtain

$$f_{p,q,\sigma}(\theta) = \frac{1}{\pi}\log\left[\frac{K_s(\theta)-K_s(q)}{K_s(\theta)-K_s(p)}\right] + \frac{1}{2\pi}\log\left[\frac{1+K_s^2(p)}{1+K_s^2(q)}\right], \quad \pi<\theta<2\pi. \tag{2.20}$$

Therefore,

$$\frac{\partial f_{p,q,\sigma}}{\partial\tau}(\theta) = \frac{\partial f_{p,q,\sigma}}{\partial\theta}(\theta) = f^2_{p,q,\sigma}(\theta),$$

for $0<p,q<\pi$, and $\pi<\theta<2\pi$ (i.e., $P,Q\in\partial\Omega^+$, but $z\in\partial\Omega^-$) if we differentiate (2.20) on both sides with respect to θ. We have proved case I.

The above calculations are based on the assumption that $\theta_\sigma = 0$. In general, suppose $\theta_\sigma \neq 0$. Through a counterclockwise rotation of angle $-\theta_\sigma$, one can first map $\Omega\backslash\sigma$ to another auxiliary domain which has the crack positioned on the positive real axis. The effect of this rotation on the conformal transform is equivalent to a translation by $-\theta_\sigma$ units on the factor K_s. So when reflected on the boundary measurement $\frac{\partial f_{p,q,\sigma}}{\partial\tau}(\theta)$, it is natural to come up with the results given in (1.3). □

To prove Theorem 2, we need the following result :

Lemma 2.1. *Assume $0 < p - \theta < \pi/2$. Then for any fixed p and θ, $\psi_j(\theta, x)$ is a continuous, nonnegative, and decreasing funtion of x on $[0, 2)$, where $j = 1, 3$. And $\psi_2(\theta, x, y)$ is a continuous, nonnegative, and decreasing funtion of x and increasing function of y on $[0, 2) \times [0, 2)$. As a result, for fixed p and θ_σ, $\alpha(p, \theta_\sigma, s_b)$ is a continuous, nonnegative, and increasing function of s_b on $[0, 2)$.*

Proof. Continuities are trivial. To show that ψ_j $(j = 1, 2, 3)$ and $\alpha(p, \theta_\sigma, s_b)$ are nonnegative, it suffices to show that

$$\text{(2.21)} \qquad \begin{cases} \left|\tan\left(\frac{m-\theta}{2}\right)\right| \geq \left|\tan\left(\frac{m_\sigma-\theta}{2}\right)\right|, \\ \left|\tan\left(\frac{m-\theta}{2}\right)\right| \geq \left|\tan\left(\frac{p-\theta}{2}\right)\right|, \\ \left|\tan\left(\frac{q-\theta}{2}\right)\right| \geq \left|\tan\left(\frac{p-\theta}{2}\right)\right|, \\ \left|\tan\left(\frac{q-\theta}{2}\right)\right| \geq \left|\tan\left(\frac{m_\sigma-\theta}{2}\right)\right|. \end{cases}$$

It requires only some algebra to check (2.21) under the assumption $0 < p-\theta < \pi/2$. All the remaining properties stated in the lemma are also the results by applying (2.21) to the definitions of the functions. □

Corollary 2.2. *Assume $0 < p - \theta < \pi/2$. Then given any σ and p, $\lambda_{\sigma,p}(\theta, \cdot)$ is decreasing on $[0, 2)$ for any fixed θ.*

Proof. Since $2\sqrt{x}/(1 + \sqrt{x})$ is an increasing function of $x \geq 0$, Lemma 2.1 implies $\lambda_{\sigma,p}(\theta, s_b)$ is decreasing with s_b on $[0, 2)$ because that $\alpha(p, \theta_\sigma, s_b)$ is increasing with s_b on $[0, 2)$. □

Now, we prove Theorem 2.

Proof of Theorem 2. Let $\partial\Omega^+$ and $\partial\Omega^-$ be defined as in Theorem 1. According to Theorem 1, we have

$$\text{(2.22)} \qquad \gamma_{p,\theta_\sigma}(s) := \left|\frac{\partial f_{p,q,\sigma}}{\partial \tau}(m)\right| \Big/ \left|\frac{\partial f_{p,q,\sigma}}{\partial \tau}(m_\sigma)\right|$$

$$= \begin{cases} \frac{|f^3_{p,q,\sigma}(m)|}{|f^4_{p,q,\sigma}(m_\sigma)|}, & \text{if M and P are both on } \partial\Omega^+ \text{ (or both on } \partial\Omega^-), \\ \frac{|f^4_{p,q,\sigma}(m)|}{|f^3_{p,q,\sigma}(m_\sigma)|}, & \text{if } M_s \text{ and P are both on } \partial\Omega^+ \text{ (or both on } \partial\Omega^-). \end{cases}$$

We will only prove the case where M and P are both on $\partial\Omega^+$. The analysis is similar for the othe cases. Without loss of generality, we can further assume $0 < p - \theta_\sigma \leq \pi/2$.

By (2.22) and (0.4), we have

$$\begin{aligned}\gamma_{p,\theta_\sigma}(s) :=& \frac{\left|f^3_{p,q,\sigma}(m)\right|}{\left|f^4_{p,q,\sigma}(m_\sigma)\right|} \\ =& \left|\frac{\tan\left(\frac{m-\theta_\sigma}{2}\right)\sec^2\left(\frac{m-\theta_\sigma}{2}\right)}{\tan\left(\frac{m_\sigma-\theta_\sigma}{2}\right)\sec^2\left(\frac{m_\sigma-\theta_\sigma}{2}\right)}\right| \cdot \left|\frac{K_s(m_\sigma-\theta_\sigma)}{K_s(m-\theta_\sigma)}\right| \cdot \\ & \left|\frac{[K_s(m_\sigma-\theta_\sigma)+K_s(p-\theta_\sigma)][K_s(m_\sigma-\theta_\sigma)-K_s(q-\theta_\sigma)]}{[K_s(m-\theta_\sigma)-K_s(p-\theta_\sigma)][K_s(m-\theta_\sigma)+K_s(q-\theta_\sigma)]}\right|.\end{aligned} \tag{2.23}$$

Rearranging the last expression and applying (1.6) - (1.9), (2.23) reads

$$\gamma_{p,\theta_\sigma}(s) = A_{p,\theta_\sigma}(s) \cdot B_{p,\theta_\sigma}(s) \cdot C_{p,\theta_\sigma}(s) \cdot D_{p,\theta_\sigma}. \tag{2.24}$$

Through some calculations, we obtain

$$\begin{aligned}\frac{\partial A_{p,\theta_\sigma}}{\partial s}(s) &= \frac{2s}{(2-s)^3} \cdot \frac{[K_s(q-\theta_\sigma)-K_s(m_\sigma-\theta_\sigma)]^2}{K_s(m_\sigma-\theta_\sigma)K_s(q-\theta_\sigma)} \\ &= \frac{2s}{(2-s)^3} \cdot \psi_1(\theta_\sigma, s),\end{aligned} \tag{2.25}$$

$$\begin{aligned}\frac{\partial B_{p,\theta_\sigma}}{\partial s}(s) =& \frac{2s}{(2-s)^3} \cdot \frac{K_s(p-\theta_\sigma)+K_s(m_\sigma-\theta_\sigma)}{K_s(m-\theta_\sigma)+K_s(q-\theta_\sigma)} \cdot \\ & \frac{K_s(m-\theta_\sigma)K_s(q-\theta_\sigma)-K_s(m_\sigma-\theta_\sigma)K_s(p-\theta_\sigma)}{K_s(m-\theta_\sigma)K_s(m_\sigma-\theta_\sigma)K_s(p-\theta_\sigma)K_s(q-\theta_\sigma)} \\ =& \frac{2s}{(2-s)^3} \cdot \psi_2(\theta_\sigma, s, s),\end{aligned} \tag{2.26}$$

and

$$\begin{aligned}\frac{\partial C_{p,\theta_\sigma}}{\partial s}(s) =& \frac{2s}{(2-s)^3} \cdot \frac{1}{K_s^3(m-\theta_\sigma)K_s(p-\theta_\sigma)} \\ =& \frac{2s}{(2-s)^3} \cdot \psi_3(\theta_\sigma, s).\end{aligned} \tag{2.27}$$

Lemma 2.1 implies that $\frac{\partial A_{p,\theta_\sigma}}{\partial s}(s) \geq 0$, $\frac{\partial B_{p,\theta_\sigma}}{\partial s}(s) \geq 0$, and $\frac{\partial C_{p,\theta_\sigma}}{\partial s}(s) \geq 0$. Hence $A_{p,\theta_\sigma}(s)$, $B_{p,\theta_\sigma}(s)$, and $C_{p,\theta_\sigma}(s)$ are increasing functions of s. Consequently, $\gamma_{p,\theta_\sigma}(s)$ is an increasing function of s due to (2.24).

To prove the rest of the theorem, next we take Taylor's expansion of $A_{p,\theta_\sigma}(s)$ around 0 and apply (2.25):

$$\begin{aligned}A_{p,\theta_\sigma}(s) &= A_{p,\theta_\sigma}(0) + \left.\frac{\partial A_{p,\theta_\sigma}}{\partial t}(t)\right|_{t=\xi_1(s)} \cdot s \\ &= a + \frac{2\xi_1(s)}{(2-\xi_1(s))^3} \cdot \psi_1(\theta_\sigma, \xi_1(s)) \cdot s,\end{aligned} \tag{2.28}$$

for some $\xi_1(s)$ between 0 and s. Since $\psi_1(\theta_\sigma, \cdot)$ is decreasing on $[0, 2)$ (Lemma 2.1), hence

$$\psi_1(\theta_\sigma, \xi_1(s)) < \psi_1(\theta_\sigma, 0) = \Psi_1. \tag{2.29}$$

From (2.28) and (2.29), we obtain

$$\begin{aligned} A_{p,\theta_\sigma}(s) &< a + \frac{2\xi_1(s)}{(2-\xi_1(s))^3} \cdot \Psi_1 \cdot s \\ &< a + \frac{2s^2}{(2-s)^3} \cdot \Psi_1. \end{aligned} \tag{2.30}$$

Similarly, we decompose $B_{p,\theta_\sigma}(s)$ and $C_{p,\theta_\sigma}(s)$ by taking their Taylor's expansions around 0 and followed by applying (2.26) and (2.27) respectively. There exist $\xi_2(s)$ and $\xi_3(s)$, so that $0 < \xi_2(s), \xi_3(s) < s$, and

$$\begin{aligned} B_{p,\theta_\sigma}(s) &= B_{p,\theta_\sigma}(0) + \frac{2\xi_2(s)}{(2-\xi_2(s))^3} \cdot \psi_2(\theta_\sigma, \xi_2(s), \xi_2(s)) \cdot s \\ &< b + \frac{2s^2}{(2-s)^3} \cdot \psi_2(\theta_\sigma, 0, s_b) = b + \frac{2s^2}{(2-s)^3} \cdot \Psi_2, \end{aligned} \tag{2.31}$$

and

$$\begin{aligned} C_{p,\theta_\sigma}(s) &= C_{p,\theta_\sigma}(0) + \frac{2\xi_3(s)}{(2-\xi_3(s))^3} \cdot \psi_3(\theta_\sigma, \xi_3(s)) \cdot s \\ &< c + \frac{2s^2}{(2-s)^3} \cdot \psi_3(\theta_\sigma, 0) = c + \frac{2s^2}{(2-s)^3} \cdot \Psi_3. \end{aligned} \tag{2.32}$$

The inequalities in (2.31) and (2.32) are based on Lemma 2.1 which states that $\psi_2(\theta_\sigma, x, y)$ is decreasing with x and increasing with y, and $\psi_3(\theta_\sigma, x)$ is decreasing with x. Now, we substitute the expressions on the RHS of (2.28), (2.31), and (2.32) for $A_{p,\theta_\sigma}(s)$, $B_{p,\theta_\sigma}(s)$, and $C_{p,\theta_\sigma}(s)$ respectively. (2.24) reads

$$\gamma_{p,\theta_\sigma}(s) = abcd + \sum_{j=1}^{3} g_j s^j, \tag{2.33}$$

where

$$\begin{aligned} g_1 =& \frac{2\xi_2(s)}{(2-\xi_2(s))^3} \cdot acd\psi_2(\theta_\sigma, \xi_2(s), \xi_2(s)) + \frac{2\xi_1(s)}{(2-\xi_1(s))^3} \cdot bcd\psi_1(\theta_\sigma, \xi_1(s)) \\ &+ \frac{2\xi_3(s)}{(2-\xi_3(s))^3} \cdot abd\psi_3(\theta_\sigma, \xi_3(s)), \\ g_2 =& \frac{2\xi_1(s)}{(2-\xi_1(s))^3} \cdot \frac{2\xi_2(s)}{(2-\xi_2(s))^3} \cdot cd\psi_1(\theta_\sigma, \xi_1(s))\psi_2(\theta_\sigma, \xi_2(s), \xi_2(s)) + \\ & \frac{2\xi_2(s)}{(2-\xi_2(s))^3} \cdot \frac{2\xi_3(s)}{(2-\xi_3(s))^3} \cdot ad\psi_2(\theta_\sigma, \xi_2(s), \xi_2(s))\psi_3(\theta_\sigma, \xi_3(s)) + \\ & \frac{2\xi_1(s)}{(2-\xi_1(s))^3} \cdot \frac{2\xi_3(s)}{(2-\xi_3(s))^3} \cdot bd\psi_1(\theta_\sigma, \xi_1(s))\psi_3(\theta_\sigma, \xi_3(s)), \\ g_3 =& \frac{2\xi_1(s)}{(2-\xi_1(s))^3} \cdot \frac{2\xi_1(s)}{(2-\xi_1(s))^3} \cdot \frac{2\xi_3(s)}{(2-\xi_3(s))^3} \cdot d \cdot \\ & \psi_1(\theta_\sigma, \xi_1(s))\psi_2(\theta_\sigma, \xi_2(s), \xi_2(s))\psi_3(\theta_\sigma, \xi_3(s)). \end{aligned} \tag{2.34}$$

Note that each $g_j \geq 0$ (by Lemma 2.1). By applying the estimates (2.30), (2.31) and (2.32) to (2.24), we obtain

$$g_1 < \frac{2s}{(2-s)^2} \cdot d(bc\Psi_1 + ac\Psi_2 + ab\Psi_3) \tag{2.35}$$

$$g_2 < \frac{4s^2}{(2-s)^6} \cdot d(c\Psi_1\Psi_2 + a\Psi_2\Psi_3 + b\Psi_1\Psi_3) \tag{2.36}$$

$$g_3 < \frac{8s^3}{(2-s)^9} \cdot d\Psi_1\Psi_2\Psi_3 \tag{2.37}$$

Let

$$\eta_{p,\theta_\sigma}(s) := g_1 + g_2 \cdot s + g_3 \cdot s^2. \tag{2.38}$$

Then $\eta_{p,\theta_\sigma}(s) \geq 0$. Since $abcd = 1$ (easy to check), (2.33) can be written as

$$\gamma_{p,\theta_\sigma}(s) = 1 + \eta_{p,\theta_\sigma}(s) \cdot s.$$

if we replace $\eta_{p,\theta_\sigma}(s)$ for $g_1 + g_2 \cdot s + g_3 \cdot s^2$. Applying (2.35), (2.36), and (2.37) to (2.38), it follows that

$$\begin{aligned}
\eta_{p,\theta_\sigma}(s) \leq & \frac{s}{(2-s)^2} \cdot \frac{2d}{2-s_b}(bc\varphi_1 + ac\varphi_2 + ab\varphi_3) + \\
& \frac{s}{(2-s)^2} \cdot \frac{4s_b^2 d}{(2-s_b)^4}(c\varphi_1\varphi_2 + a\varphi_2\varphi_3 + b\varphi_1\varphi_3) \\
& + \frac{s}{(2-s)^2} \cdot \frac{8s_b^4 d}{(2-s_b)^7}\varphi_1\varphi_2\varphi_3 \\
= & \frac{s}{(2-s)^2} \cdot \alpha(p, \theta_\sigma, s_b),
\end{aligned}$$

This completes the proof. □

3. Proof of Theorem 3. To show $Q_j \to z_\sigma$, as $j \to \infty$, it suffices to show $\measuredangle Q_j O z_\sigma \le \frac{\pi}{2^j}$ for all j. We would like to prove (by induction) that

$$\measuredangle Q_j O z_\sigma \le \measuredangle Q_{j-1} O Q_j = \frac{\pi}{2^j} \tag{3.1}$$

for all $j = 1, 2, 3, \cdots$.

z_σ lies either on $\overset{\frown}{P_0 Q_0}$ or on $\overset{\frown}{Q_0 P_0}$. It is trivial that $\measuredangle Q_0 O z_\sigma \le \measuredangle Q_0 O P_0 = \pi$. If $z_\sigma \in \overset{\frown}{P_0 Q_0}$, then $|\frac{\partial f}{\partial \tau}(r_0)| < |\frac{\partial f}{\partial \tau}(n_0)|$. According to (2) in the algorithm, Q_1 is obtained by rotating Q_0 clockwise through an angle of $\frac{\pi}{2}$. In other words, either $z_\sigma \in \overset{\frown}{P_0 Q_1}$ or $z_\sigma \in \overset{\frown}{Q_1 Q_0}$. Similar argument applies for the case where $z_\sigma \in \overset{\frown}{Q_0 P_0}$. So when $j = 1$,

$$\measuredangle Q_1 O z_\sigma \le \measuredangle Q_0 O Q_1 = \frac{\pi}{2}.$$

Assume (3.1) holds for $j = k$. We have to prove that (3.1) is also true for $j = k+1$. There are two possibilities:

Case I : $|\frac{\partial f}{\partial \tau}(r_k)| > |\frac{\partial f}{\partial \tau}(n_k)|$. Following (1) in the algorithm, Q_{k+1} is obtained by rotating Q_k counterclockwise through an angle of $\frac{\pi}{2^{k+1}}$. In other words, $\measuredangle Q_k O Q_{k+1} = \frac{\pi}{2^{k+1}}$. From the claim preceding Theorem 2, we know that $z_\sigma \in \overset{\frown}{Q_k P_k}$. Hence either $z_\sigma \in \overset{\frown}{Q_k Q_{k+1}}$ or $z_\sigma \in \overset{\frown}{Q_{k+1} P_k}$. In case $z_\sigma \in \overset{\frown}{Q_k Q_{k+1}}$, then obviously

$$\measuredangle Q_{k+1} O z_\sigma \le \measuredangle Q_k O Q_{k+1} = \frac{\pi}{2^{k+1}}.$$

If $z_\sigma \in \overset{\frown}{Q_{k+1} P_k}$, i.e., $Q_{k+1} \in \overset{\frown}{Q_k z_\sigma}$, then

$$\measuredangle Q_{k+1} O z_\sigma = \measuredangle Q_k O z_\sigma - \measuredangle Q_k O Q_{k+1}. \tag{3.2}$$

Since the induction hypothesis implies that

$$\measuredangle Q_k O z_\sigma \le \measuredangle Q_{k-1} O Q_k = \frac{\pi}{2^k}$$

and

$$\measuredangle Q_k O Q_{k+1} = \frac{1}{2} \measuredangle Q_{k-1} O Q_k = \frac{\pi}{2^{k+1}},$$

therefore from (3.2), we obtain

$$\begin{aligned} \measuredangle Q_{k+1} O z_\sigma &\le \measuredangle Q_{k-1} O Q_k - \measuredangle Q_k O Q_{k+1} \\ &= 2 \measuredangle Q_k O Q_{k+1} - \measuredangle Q_k O Q_{k+1} \\ &= \measuredangle Q_k O Q_{k+1} = \frac{\pi}{2^{k+1}}. \end{aligned} \tag{3.3}$$

Case II : $|\frac{\partial f}{\partial \tau}(M_k)| < |\frac{\partial f}{\partial \tau}(N_k)|$. following (1) of the algorithm, one obtains Q_{k+1} by rotating Q_k clockwise through an angle of $\frac{\pi}{2^{k+1}}$. Again, $\measuredangle Q_k O Q_{k+1} = \frac{\pi}{2^{k+1}}$.

Now, it must true that $z_\sigma \in \widehat{P_k Q_k}$ and this implies that either $z_\sigma \in \widehat{P_k Q_{k+1}}$ or $z_\sigma \in \widehat{Q_{k+1} Q_k}$. In case $z_\sigma \in \widehat{Q_{k+1} Q_k}$, then clearly

$$\angle Q_{k+1} O z_\sigma \leq \angle Q_{k+1} O Q_k = \frac{\pi}{2^{k+1}}.$$

Otherwise suppose $z_\sigma \in \widehat{P_k Q_{k+1}}$, i.e., $Q_{k+1} \in \widehat{z_\sigma Q_k}$. Then (3.2) still holds. The rest of the argument is nothing different from Case I. So we conclude that (3.1) is true for $j = k+1$. □

To prove Theorem 4, we need the following preliminary results.

Lemma 3.1. *Suppose* $0 < s < s_b < 2$. $\gamma_{p,\theta_\sigma}(s)$ *and* $\alpha(p, \theta_\sigma, s_b)$ *are defined as in Theorem 2. Then*

$$s > \lambda_{\sigma,p}(\theta_\sigma, s_b) > 0 \tag{3.4}$$

for $0 < p - \theta_\sigma \leq \pi/2$.

Proof. By substituting (1.6) into (1.2) and solving the resulting inequality for s, we obtain

$$s > 2\sqrt{\frac{\gamma_{p,\theta_\sigma}(s) - 1}{\alpha(p, \theta_\sigma, s_b)}} \Bigg/ \left(1 + \sqrt{\frac{\gamma_{p,\theta_\sigma}(s) - 1}{\alpha(p, \theta_\sigma, s_b)}}\right) = \lambda_{\sigma,p}(\theta_\sigma, s_b)$$

The second inequality immediately follows since $\gamma_{p,\theta_\sigma}(s) > 1$.

Lemma 3.2. *Assume* $0 < p - \theta < \pi/2$. *Then for any fixed* p *and* θ, $\phi_j(\theta, x, y)$ *is a continuous, nonnegative, and decreasing funtion of* x *and increasing function of* y *on* $[0, 2) \times [0, 2)$, *where* $j = 1, 2, 3$. *As a result, for fixed* p *and* θ_σ, $\beta(p, \theta_\sigma, s_{lb}, s_b)$ *is a continuous, nonnegative, and decreasing function of* s_{lb} *and increasing function of* s_b *on* $[0, 2) \times [0, 2)$.

Proof. Similar to the proof for Lemma 2.1. □

Lemma 3.3. *Let* $A_{p,\theta_\sigma}(s)$, $B_{p,\theta_\sigma}(s)$, $C_{p,\theta_\sigma}(s)$, *and* $D_{p,\theta_\sigma}(s)$ *be defined as in (1.6), (1.7), (1.8), and (1.9) respectively. Denote*

$$\begin{cases} A = A_{p,\theta_\sigma}(s_b), \\ B = B_{p,\theta_\sigma}(s_b), \\ C = C_{p,\theta_\sigma}(s_b), \\ D = D_{p,\theta_\sigma}, \end{cases} \tag{3.5}$$

and let

$$\Phi_j = \phi_j(\theta_\sigma, s_{lb}, s_b), \quad j = 1,2,3. \tag{3.6}$$

Assume $0 < p - \theta_\sigma < \pi/2$, *and* $0 < s_{lb} \le s < s_b \le 1$. *Then*

$$s < s_b - \frac{\gamma_{p,\theta_\sigma}(s_b) - \gamma_{p,\theta_\sigma}(s)}{\beta(p, \theta_\sigma, s_{lb}, s_b)} \tag{3.7}$$

if $s \ge \max\left\{s_b - \frac{A}{\Phi_1}, s_b - \frac{B}{\Phi_2}, s_b - \frac{C}{\Phi_3}\right\}$.

Proof. Take Taylor's expansion of $A_{p,\theta_\sigma}(s)$ around s_b :

$$A_{p,\theta_\sigma}(s) = A_{p,\theta_\sigma}(s_b) + \left.\frac{\partial A_{p,\theta_\sigma}}{\partial s}(s)\right|_{s=\zeta_1} \cdot (s - s_b) \tag{3.8}$$

for some ζ_1, s.t. $s < \zeta_1 < s_b$. From (1.17),

$$\begin{aligned} \left.\frac{\partial A_{p,\theta_\sigma}}{\partial t}(t)\right|_{t=\zeta_1} &= \frac{2\zeta_1}{(2-\zeta_1)^3} \cdot \frac{[K_{\zeta_1}(q-\theta_\sigma) - K_{\zeta_1}(m_\sigma - \theta_\sigma)]^2}{K_{\zeta_1}(m_\sigma - \theta_\sigma) K_{\zeta_1}(q - \theta_\sigma)} \\ &= \phi_1(\theta_\sigma, \zeta_1, \zeta_1) \end{aligned} \tag{3.9}$$

if $0 < p - \theta_\sigma < \pi/2$. Since $0 < s_{lb} < s < \zeta_1 < s_b < 2$, Lemma 3.2 implies that

$$\phi_1(\theta_\sigma, \zeta_1, \zeta_1) < \phi_1(\theta_\sigma, s_{lb}, s_b). \tag{3.10}$$

Suppose $s \ge \max\left\{s_b - \frac{A}{\Phi_1}, s_b - \frac{B}{\Phi_2}, s_b - \frac{C}{\Phi_3}\right\}$, then applying (3.9) and (3.10) to (3.8), we obtain the following estimate

$$\begin{aligned} A_{p,\theta_\sigma}(s) &> A_{p,\theta_\sigma}(s_b) + \phi_1(\theta_\sigma, s_{lb}, s_b) \cdot (s - s_b) \\ &= A + \Phi_1 \cdot (s - s_b) \ge 0 \end{aligned} \tag{3.11}$$

if $s_{lb} < s < s_b$. Similarly,

$$\begin{aligned} B_{p,\theta_\sigma}(s) &> B_{p,\theta_\sigma}(s_b) + \phi_2(\theta_\sigma, s_{lb}, s_b) \cdot (s - s_b) \\ &= B + \Phi_2 \cdot (s - s_b) \ge 0 \end{aligned} \tag{3.12}$$

and

$$\begin{aligned} C_{p,\theta_\sigma}(s) &> C_{p,\theta_\sigma}(s_b) + \phi_3(\theta_\sigma, s_{lb}, s_b) \cdot (s - s_b) \\ &= C + \Phi_3 \cdot (s - s_b) \ge 0 \end{aligned} \tag{3.13}$$

if $s_{lb} < s < s_b$. Recall that from (2.24),

$$\gamma_{p,\theta_\sigma}(s) = A_{p,\theta_\sigma}(s) \cdot B_{p,\theta_\sigma}(s) \cdot C_{p,\theta_\sigma}(s) \cdot D_{p,\theta_\sigma}. \tag{2.24}$$

Applying the estimates (3.11), (3.12), and (3.13) to (2.24), we have

$$\begin{aligned} \gamma_{p,\theta_\sigma}(s) >& [A + \Phi_1 \cdot (s - s_b)] \cdot [B + \Phi_2 \cdot (s - s_b)] \cdot [C + \Phi_3 \cdot (s - s_b)] \cdot D \\ =& ABCD + \widetilde{\eta}_{p,\theta_\sigma}(s) = \gamma_{p,\theta_\sigma}(s_b) + \widetilde{\eta}_{p,\theta_\sigma}(s), \end{aligned} \tag{3.14}$$

where

(3.15)

$$\widetilde{\eta}_{p,\theta_\sigma}(s) = (ABD\Phi_3 + ACD\Phi_2 + BCD\Phi_1)(s - s_b) + (AD\Phi_2\Phi_3 + BD\Phi_1\Phi_3 + CD\Phi_1\Phi_2)(s - s_b)^2 + D\Phi_1\Phi_2\Phi_3 \cdot (s - s_b)^3$$

Since $s_b < 1$, $0 < s < s_b$ implies that

$$s - s_b < (s - s_b)^3. \tag{3.16}$$

Applying (3.16) to (3.15), we obtain

$$\begin{aligned} \widetilde{\eta}_{p,\theta_\sigma}(s) &> (ABD\Phi_3 + ACD\Phi_2 + BCD\Phi_1)(s - s_b) + D\Phi_1\Phi_2\Phi_3 \cdot (s - s_b) \\ &= \beta(p, \theta_\sigma, s_{lb}, s_b) \cdot (s - s_b). \end{aligned} \tag{3.17}$$

for $A, B, C, D > 0$, and $\Phi_j > 0$, $\forall j = 1, 2, 3$. Using (3.17), (3.14) reads

$$\gamma_{p,\theta_\sigma}(s) > \gamma_{p,\theta_\sigma}(s_b) + \beta(p, \theta_\sigma, s_{lb}, s_b) \cdot (s - s_b). \tag{3.18}$$

The result (3.7) immediately follows by solving (3.18) for s. □

Lemma 3.4. *Assume* $0 < p - \theta_\sigma < \pi/2$ *and* $1 < s_b < 2$. $\beta(p, \theta_\sigma, s_{lb}, s_b)$ *is defined in (1.18). If* $0 < s_{lb} \le s < s_b$, *then*

(1) *for* $s \ge s_b - 1$,

$$s < s_b - \frac{\gamma_{p,\theta_\sigma}(s_b) - \gamma_{p,\theta_\sigma}(s)}{\beta(p, \theta_\sigma, \tilde{s}_{lb}, s_b)}, \tag{3.19}$$

if $s \ge \max\left\{s_b - \frac{A}{\widetilde{\Phi}_1}, s_b - \frac{B}{\widetilde{\Phi}_2}, s_b - \frac{C}{\widetilde{\Phi}_3}\right\}$, *where* $\tilde{s}_{lb} = \max(s_{lb}, s_b - 1)$, *and*

$$\widetilde{\Phi}_j = \phi_j(\theta_\sigma, \tilde{s}_{lb}, s_b), \quad j = 1,2,3.$$

(2) *for* $s < s_b - 1$,

$$s < \min\left(s_b - 1, \sqrt[3]{\frac{\gamma_{p,\theta_\sigma}(s_b) - \gamma_{p,\theta_\sigma}(s)}{\beta(p, \theta_\sigma, s_{lb}, s_b)}}\right). \tag{3.19'}$$

if $s \ge \max\left\{s_b - \frac{A}{\Phi_1}, s_b - \frac{B}{\Phi_2}, s_b - \frac{C}{\Phi_3}\right\}$.

Proof. (1) Note that from the proof for Lemma 3.3, (3.7) is valid for any pair of $\{s_{lb}, s_b\}$ which satisfies $0 < s_{lb} \le s < s_b < 2$ and (3.16) if furthermore,

$$s \ge \max\left\{s_b - \frac{A}{\phi_1(\theta_\sigma, s_{lb}, s_b)}, s_b - \frac{B}{\phi_2(\theta_\sigma, s_{lb}, s_b)}, s_b - \frac{C}{\phi_3(\theta_\sigma, s_{lb}, s_b)}\right\}. \tag{3.20}$$

Since $s_{lb} \le s$ and $s \ge s_b - 1$, we have $0 < \tilde{s}_{lb} \le s < s_b$. Moreover,

$$s \ge s_b - 1 \Longrightarrow -1 \le s - s_b \le (s - s_b)^3 < 0.$$

Therefore (3.16) holds. (3.19) immediately follows by replacing the new lower bound $\tilde{s}_{lb}$ for s_{lb} in Lemma 3.3 and the condition (3.20).

(2) For $s < s_b - 1$, (3.8) – (3.15) are still valid if $s \geq \max\left\{s_b - \frac{A}{\Phi_1}, s_b - \frac{B}{\Phi_2}, s_b - \frac{C}{\Phi_3}\right\}$. Moreover, $s < s_b - 1$ implies

$$(s - s_b)^3 < s - s_b < -1. \tag{3.21}$$

From (3.15) and (3.21), we obtain the following lower bound for $\widetilde{\eta}_{p,\theta_\sigma}(s)$:

(3.22)

$$\begin{aligned}\widetilde{\eta}_{p,\theta_\sigma}(s) &> (ABD\Phi_3 + ACD\Phi_2 + BCD\Phi_1)(s - s_b)^3 + D\Phi_1\Phi_2\Phi_3 \cdot (s - s_b)^3 \\ &= \beta(p, \theta_\sigma, s_{lb}, s_b) \cdot (s - s_b)^3.\end{aligned}$$

Coupling (3.14) and (3.22) together results in the following inequality:

$$\gamma_{p,\theta_\sigma}(s) > \gamma_{p,\theta_\sigma}(s_b) + \beta(p, \theta_\sigma, s_{lb}, s_b) \cdot (s - s_b)^3.$$

Under the assumption that $s < s_b - 1$, we obtain (3.19') by solving the last inequality for s. □

Lemma 3.5. *Assume* $0 < p - \theta_\sigma < \pi/2$ *and* $0 < s_{lb} \leq s < s_b < 2$. *Then*

$$s < \omega^1_{\sigma,p}(\theta_\sigma, s_{lb}, s_b) \leq s_b \tag{3.23}$$

if $\gamma_{p,\theta_\sigma}(s) \geq \gamma_{p,\theta_\sigma}\left(\omega^2_p(\theta_\sigma, s_{lb}, s_b)\right)$ *or* $\omega^2_p(\theta_\sigma, s_{lb}, s_b) < 0$.

Proof. Suppose $\omega^2_p(\theta_\sigma, s_{lb}, s_b) < 0$, obviously $s \geq \omega^2_p(\theta_\sigma, s_{lb}, s_b)$. Suppose $\omega^2_p(\theta_\sigma, s_{lb}, s_b) \geq 0$ and $\gamma_{p,\theta_\sigma}(s) \geq \gamma_{p,\theta_\sigma}\left(\omega^2_p(\theta_\sigma, s_{lb}, s_b)\right)$, then $s \geq \omega^2_p(\theta_\sigma, s_{lb}, s_b)$ since $\gamma_{p,\theta_\sigma}(\cdot)$ is increasing on $[0, 2)$. In other words, if $\gamma_{p,\theta_\sigma}(s) \geq \gamma_{p,\theta_\sigma}\left(\omega^2_p(\theta_\sigma, s_{lb}, s_b)\right)$ or $\omega^2_p(\theta_\sigma, s_{lb}, s_b) < 0$, then

$$s \geq \omega^2_p(\theta_\sigma, s_{lb}, s_b) = \max\left\{s_b - \frac{A}{\Phi_1}, s_b - \frac{B}{\Phi_2}, s_b - \frac{C}{\Phi_3}\right\}. \tag{3.24}$$

There are three cases:

$$\begin{aligned}&\text{Case I}: && s_b \leq 1, \\ &\text{Case II}: && s_b > 1 \quad \text{and} \quad s \geq s_b - 1, \\ &\text{Case III}: && s_b > 1 \quad \text{and} \quad s \leq s_b - 1.\end{aligned}$$

First of all, we claim that for Case I and Case II,

$$s < \min\left\{s_b - \frac{\gamma_{p,\theta_\sigma}(s_b) - \gamma_{p,\theta_\sigma}(s)}{\beta(p, \theta_\sigma, s_{lb}, s_b)}, s_b - \frac{\gamma_{p,\theta_\sigma}(s_b) - \gamma_{p,\theta_\sigma}(s)}{\beta(p, \theta_\sigma, \tilde{s}_{lb}, s_b)}\right\}. \tag{3.25}$$

if $\gamma_{p,\theta_\sigma}(s) \geq \gamma_{p,\theta_\sigma}\left(\omega^2_p(\theta_\sigma, s_{lb}, s_b)\right)$ or $\omega^2_p(\theta_\sigma, s_{lb}, s_b) < 0$.

Proof of (3.25) : When $s_b \leq 1$, we have shown in Lemma 3.3 that (3.7) is true if (3.24) holds. Hence,

$$s < s_b - \frac{\gamma_{p,\theta_\sigma}(s_b) - \gamma_{p,\theta_\sigma}(s)}{\beta(p, \theta_\sigma, s_{lb}, s_b)}. \tag{3.7}$$

if $\gamma_{p,\theta_\sigma}(s) \geq \gamma_{p,\theta_\sigma}\left(\omega_p^2(\theta_\sigma, s_{lb}, s_b)\right)$ or $\omega_p^2(\theta_\sigma, s_{lb}, s_b) < 0$. Since,

$$s_b \leq 1 \Longrightarrow s_b - 1 \leq 0 \Longrightarrow \tilde{s}_{lb} = s_{lb},$$

therefore,

$$\begin{aligned} &\min\left\{ s_b - \frac{\gamma_{p,\theta_\sigma}(s_b) - \gamma_{p,\theta_\sigma}(s)}{\beta(p, \theta_\sigma, s_{lb}, s_b)}, s_b - \frac{\gamma_{p,\theta_\sigma}(s_b) - \gamma_{p,\theta_\sigma}(s)}{\beta(p, \theta_\sigma, \tilde{s}_{lb}, s_b)} \right\} \\ =& s_b - \frac{\gamma_{p,\theta_\sigma}(s_b) - \gamma_{p,\theta_\sigma}(s)}{\beta(p, \theta_\sigma, s_{lb}, s_b)} \\ =& s_b - \frac{\gamma_{p,\theta_\sigma}(s_b) - \gamma_{p,\theta_\sigma}(s)}{\beta(p, \theta_\sigma, \tilde{s}_{lb}, s_b)}. \end{aligned} \tag{3.26}$$

By (3.7) and (3.26), we obtain (3.25) in case $s_b \leq 1$ and this proves (3.25) for Case I.

When $s_b > 1$ and $s \geq s_b - 1$, Lemma 3.4 (1) implies (3.19) if (3.24) is valid. That is,

$$s < s_b - \frac{\gamma_{p,\theta_\sigma}(s_b) - \gamma_{p,\theta_\sigma}(s)}{\beta(p, \theta_\sigma, \tilde{s}_{lb}, s_b)} \tag{3.19}$$

when $\gamma_{p,\theta_\sigma}(s) \geq \gamma_{p,\theta_\sigma}\left(\omega_p^2(\theta_\sigma, s_{lb}, s_b)\right)$ or $\omega_p^2(\theta_\sigma, s_{lb}, s_b) < 0$. If $s_{lb} \geq s_b - 1$, then $\tilde{s}_{lb} = s_{lb}$. Hence (3.26) holds when $s_{lb} \geq s_b - 1$. By (3.19) and (3.26), we have once again proved (3.25) for $s_{lb} \geq s_b - 1$. Suppose $s_{lb} < s_b - 1$, then $\tilde{s}_{lb} = s_b - 1$. Since $\beta(p, \theta_\sigma, s_{lb}, s_b)$ is decreasing with s_{lb} on [0,2) for any fixed p, θ_σ, and s_b (Lemma 3.2), therefore

$$s_{lb} < s_b - 1 \Longrightarrow s_b - \frac{\gamma_{p,\theta_\sigma}(s_b) - \gamma_{p,\theta_\sigma}(s)}{\beta(p, \theta_\sigma, s_{lb}, s_b)} \geq s_b - \frac{\gamma_{p,\theta_\sigma}(s_b) - \gamma_{p,\theta_\sigma}(s)}{\beta(p, \theta_\sigma, s_b - 1, s_b)}.$$

So,

$$\begin{aligned} &\min\left\{ s_b - \frac{\gamma_{p,\theta_\sigma}(s_b) - \gamma_{p,\theta_\sigma}(s)}{\beta(p, \theta_\sigma, s_{lb}, s_b)}, s_b - \frac{\gamma_{p,\theta_\sigma}(s_b) - \gamma_{p,\theta_\sigma}(s)}{\beta(p, \theta_\sigma, \tilde{s}_{lb}, s_b)} \right\} \\ =& s_b - \frac{\gamma_{p,\theta_\sigma}(s_b) - \gamma_{p,\theta_\sigma}(s)}{\beta(p, \theta_\sigma, s_b - 1, s_b)} \\ =& s_b - \frac{\gamma_{p,\theta_\sigma}(s_b) - \gamma_{p,\theta_\sigma}(s)}{\beta(p, \theta_\sigma, \tilde{s}_{lb}, s_b)} \end{aligned} \tag{3.27}$$

for $s_{lb} < s_b - 1$, if $\gamma_{p,\theta_\sigma}(s) \geq \gamma_{p,\theta_\sigma}\left(\omega_p^2(\theta_\sigma, s_{lb}, s_b)\right)$ or $\omega_p^2(\theta_\sigma, s_{lb}, s_b) < 0$. By (3.19) and (3.27), we see that

$$s < \min\left\{ s_b - \frac{\gamma_{p,\theta_\sigma}(s_b) - \gamma_{p,\theta_\sigma}(s)}{\beta(p, \theta_\sigma, s_{lb}, s_b)}, s_b - \frac{\gamma_{p,\theta_\sigma}(s_b) - \gamma_{p,\theta_\sigma}(s)}{\beta(p, \theta_\sigma, \tilde{s}_{lb}, s_b)} \right\}$$

for $s_{lb} < s_b - 1$ if $\gamma_{p,\theta_\sigma}(s) \geq \gamma_{p,\theta_\sigma}\left(\omega_p^2(\theta_\sigma, s_{lb}, s_b)\right)$ or $\omega_p^2(\theta_\sigma, s_{lb}, s_b) < 0$. This completes the proof of (3.25) for Case II.

As for Case III, we have shown in Lemma 3.4 (2) that (3.19') holds. The first inequality in (3.23) follows by taking the maximum of two upper bounds of s given in (3.19') and (3.25). Moreover, we know that $\gamma_{p,\theta_\sigma}(s)$ is an increasing function of s on [0,2) (Theorem 2). Hence given any p and θ_σ, $\gamma_{p,\theta_\sigma}(s_b) > \gamma_{p,\theta_\sigma}(s)$ and this implies $\omega_{\sigma,p}(\theta_\sigma, s_{lb}, s_b) \leq s_b$. □

Proof of Theorem 4. To show (1.24), we first claim that

$$0 < t_j < s < s_j < s_b, \qquad \forall j = 0, 1, 2, ... \tag{3.28}$$

Proof of (3.28) : When $j = 0$, $s < s_0 = s_b$ from the definition (1.23). Applying Lemma 3.1, we have

$$\begin{aligned} s &> 2\sqrt{\frac{\gamma_{p,\theta_\sigma}(s) - 1}{\alpha(p, \theta_\sigma, s_0)}} \Bigg/ \left(1 + \sqrt{\frac{\gamma_{p,\theta_\sigma}(s) - 1}{\alpha(p, \theta_\sigma, s_0)}}\right) \\ &= \lambda_{\sigma,p}(\theta_\sigma, s_0) = t_0. \end{aligned}$$

So (3.28) holds when $j = 0$. Assume (3.28) is valid for $j \leq k$. That is,

$$0 < t_k < s < s_k < s_b.$$

Then by Lemma 3.5,

$$s < \omega_{\sigma,p}^1(\theta_\sigma, t_k, s_k) < s_k \tag{3.29a}$$

if $\gamma_{p,\theta_\sigma}(s) \geq \gamma_{p,\theta_\sigma}\left(\omega_p^2(\theta_\sigma, t_k, s_k)\right)$ or $\omega_p^2(\theta_\sigma, t_k, s_k) < 0$. Otherwise,

$$s < \omega_p^2(\theta_\sigma, t_k, s_k) < s_k \tag{3.29b}$$

if $\omega_p^2(\theta_\sigma, t_k, s_k) \geq 0$ and $\gamma_{p,\theta_\sigma}(s) < \gamma_{p,\theta_\sigma}\left(\omega_p^2(\theta_\sigma, t_k, s_k)\right)$, since $\gamma_{p,\theta_\sigma}(\cdot)$ is increasing on $[0, 2)$. The second inequality in (3.29b) is trivial from the definition (1.20) of ω_p^2. (3.29a) and (3.29b) simply means

$$s < \underbrace{\omega_{\sigma,p}(\theta_\sigma, t_k, s_k)}_{s_{k+1}} < s_k. \tag{3.29}$$

Under the condition (3.29) and applying Lemma 3.1 with the new upper bound s_{k+1} for s, we obtain

$$
\begin{aligned}
(3.30) \qquad s &> 2\sqrt{\frac{\gamma_{p,\theta_\sigma}(s)-1}{\alpha(p,\theta_\sigma,s_{k+1})}}\Bigg/\left(1+\sqrt{\frac{\gamma_{p,\theta_\sigma}(s)-1}{\alpha(p,\theta_\sigma,s_{k+1})}}\right) \\
&= \lambda_{\sigma,p}(\theta_\sigma,s_{k+1}) = t_{k+1} > 0.
\end{aligned}
$$

Coupling (3.29) and (3.30) together gives (3.28) for $j = k+1$. Therefore by induction, we have shown that (3.28) holds for all $j = 0, 1, 2, ...$ More than that, (3.29) is true for all $k = 0, 1, 2, ...$, i.e.,

$$
(3.31) \qquad s < \cdots < s_2 < s_1 < s_0 = s_b.
$$

To complete the proof of (1.24), it remains to show that $\{t_j\}_{j=0}^{\infty}$ is an increasing sequence. But from Corollary 2.2, we know that $\lambda_{\sigma,p}(\theta_\sigma,\cdot)$ is a decreasing function on $[0,2)$. Since $\{s_j\}_{j=0}^{\infty}$ is a decreasing sequence (by (3.31)), hence

$$
\lambda_{\sigma,p}(\theta_\sigma,s_k) < \lambda_{\sigma,p}(\theta_\sigma,s_{k+1}), \quad \forall\, k = 0,1,2,...
$$

or equivalently,

$$
t_k < t_{k+1}, \quad \forall\, k = 0,1,2,...
$$

So $\{t_j\}_{j=0}^{\infty}$ is an increasing sequence and (1.24) follows immediately.

We can proceed to prove (1.25). We know that (from (1.24)) $\exists\ t^*$ and s^*, s.t.,

$$
(3.32) \qquad t^* = \lim_{j\to\infty} t_j = \sup_j t_j, \quad \text{and} \quad s^* = \lim_{j\to\infty} s_j = \inf_j s_j.
$$

First, we would like to show that there must exist an $n_0 \in \mathbb{N}$, s.t.,

$$
(3.33) \qquad \omega_{\sigma,p}(\theta_\sigma,t_j,s_j) = \omega^1_{\sigma,p}(\theta_\sigma,t_j,s_j), \quad \forall\, j \geq n_0
$$

Suppose this is not true, then from the definition (1.22) of $\omega_{\sigma,p}$, there must exist a subsequence $\{j_k\}_{k=1}^{\infty}$, so that

$$
\omega_{\sigma,p}(\theta_\sigma,t_{j_k},s_{j_k}) = \omega^2_p(\theta_\sigma,t_{j_k},s_{j_k}), \quad \forall\, k = 1,2,3...
$$

By (1.19), we have

(3.34)

$$
\begin{aligned}
&s_{j_k+1} - s = \omega^2_p(\theta_\sigma,t_{j_k},s_{j_k}) - s \\
=&\max\left\{s_{j_k} - \frac{A_{p,\theta_\sigma}(s_{j_k})}{\phi_1(\theta_\sigma,t_{j_k},s_{j_k})},\ s_{j_k} - \frac{B_{p,\theta_\sigma}(s_{j_k})}{\phi_2(\theta_\sigma,t_{j_k},s_{j_k})},\ s_{j_k} - \frac{C_{p,\theta_\sigma}(s_{j_k})}{\phi_3(\theta_\sigma,t_{j_k},s_{j_k})}\right\} - s \\
\leq&(s_{j_k} - s) - \min\left\{\frac{A_{p,\theta_\sigma}(s_{j_k})}{\phi_1(\theta_\sigma,t_{j_k},s_{j_k})},\ \frac{B_{p,\theta_\sigma}(s_{j_k})}{\phi_2(\theta_\sigma,t_{j_k},s_{j_k})},\ \frac{C_{p,\theta_\sigma}(s_{j_k})}{\phi_3(\theta_\sigma,t_{j_k},s_{j_k})}\right\}.
\end{aligned}
$$

Note that $A_{p,\theta_\sigma}(\cdot)$, $B_{p,\theta_\sigma}(\cdot)$, and $C_{p,\theta_\sigma}(\cdot)$ are continuous on $[0,2)$. $\phi_j(\theta_\sigma,\cdot,\cdot)$ $(j=1,2,3)$ is continuous on $[0,2)\times[0,2)$. Since (3.32) implies $\lim_{k\to\infty} s_{j_k} = s^*$ and $\lim_{k\to\infty} t_{j_k} = t^*$, passing limits on both sides of (3.34) as $k\to\infty$, we obtain

$$s^* - s \le (s^* - s) - \min\left\{\frac{A_{p,\theta_\sigma}(s^*)}{\phi_1(\theta_\sigma,t^*,s^*)}, \frac{B_{p,\theta_\sigma}(s^*)}{\phi_2(\theta_\sigma,t^*,s^*)}, \frac{C_{p,\theta_\sigma}(s^*)}{\phi_3(\theta_\sigma,t^*,s^*)}\right\}.$$

Therefore,

$$0 \ge \min\left\{\frac{A_{p,\theta_\sigma}(s^*)}{\phi_1(\theta_\sigma,t^*,s^*)}, \frac{B_{p,\theta_\sigma}(s^*)}{\phi_2(\theta_\sigma,t^*,s^*)}, \frac{C_{p,\theta_\sigma}(s^*)}{\phi_3(\theta_\sigma,t^*,s^*)}\right\}. \tag{3.35}$$

However, in Theorem 2 we have shown that

$$\gamma_{p,\theta_\sigma}(s*) = A_{p,\theta_\sigma}(s^*)\cdot B_{p,\theta_\sigma}(s^*)\cdot C_{p,\theta_\sigma}(s^*)\cdot D_{p,\theta_\sigma} \ge 1, \tag{3.36}$$

which is the result of (1.5). (3.36) simply implies that all of $A_{p,\theta_\sigma}(s^*)$, $B_{p,\theta_\sigma}(s^*)$ and $C_{p,\theta_\sigma}(s^*)$ must be greater than 0. Since each $\phi_j(\theta_\sigma,t^*,s^*)$ is nonnegative (Lemma 3.2), hence

$$0 < \min\left\{\frac{A_{p,\theta_\sigma}(s^*)}{\phi_1(\theta_\sigma,t^*,s^*)}, \frac{B_{p,\theta_\sigma}(s^*)}{\phi_2(\theta_\sigma,t^*,s^*)}, \frac{C_{p,\theta_\sigma}(s^*)}{\phi_3(\theta_\sigma,t^*,s^*)}\right\}.$$

But this contradicts (3.35). So, there must exist an $n_0\in\mathbb{N}$ so that (3.33) holds.

Now, we use the fact (3.33) and apply the formula (1.19). Then we get

$$\begin{aligned}
&s_{j+1} - s = \omega_{\sigma,p}(\theta_\sigma,t_j,s_j) - s = \omega^1_{\sigma,p}(\theta_\sigma,t_j,s_j) - s\\
&= \max\left\{\min\left\{s_j - \frac{\gamma_{p,\theta_\sigma}(s_j)-\gamma_{p,\theta_\sigma}(s)}{\beta(p,\theta_\sigma,t_j,s_j)}, s_j - \frac{\gamma_{p,\theta_\sigma}(s_j)-\gamma_{p,\theta_\sigma}(s)}{\beta(p,\theta_\sigma,\tilde{t}_j,s_j)}\right\},\right.\\
&\qquad \left.\min\left\{s_j - 1, s_j - \sqrt[3]{\frac{\gamma_{p,\theta_\sigma}(s_j)-\gamma_{p,\theta_\sigma}(s)}{\beta(p,\theta_\sigma,t_j,s_j)}}\right\}\right\} - s\\
&\le \max\left\{s_j - \frac{\gamma_{p,\theta_\sigma}(s_j)-\gamma_{p,\theta_\sigma}(s)}{\beta(p,\theta_\sigma,t_j,s_j)}, s_j - \sqrt[3]{\frac{\gamma_{p,\theta_\sigma}(s_j)-\gamma_{p,\theta_\sigma}(s)}{\beta(p,\theta_\sigma,t_j,s_j)}}\right\} - s\\
&= (s_j - s) - \min\left\{\frac{\gamma_{p,\theta_\sigma}(s_j)-\gamma_{p,\theta_\sigma}(s)}{\beta(p,\theta_\sigma,t_j,s_j)}, \sqrt[3]{\frac{\gamma_{p,\theta_\sigma}(s_j)-\gamma_{p,\theta_\sigma}(s)}{\beta(p,\theta_\sigma,t_j,s_j)}}\right\}, \quad \forall j \ge n_0.
\end{aligned}$$

Since $\gamma_{p,\theta_\sigma}(\cdot)$ is continuous on $[0,2)$ and $\beta(p,\theta_\sigma,\cdot,\cdot)$ is continuous on $[0,2)\times[0,2)$, taking limits as $j\to\infty$ on both sides of the above inequality and applying (3.32), we obtain

$$s^* - s \le (s^* - s) - \min\left\{\frac{\gamma_{p,\theta_\sigma}(s^*)-\gamma_{p,\theta_\sigma}(s)}{\beta(p,\theta_\sigma,t^*,s^*)}, \sqrt[3]{\frac{\gamma_{p,\theta_\sigma}(s^*)-\gamma_{p,\theta_\sigma}(s)}{\beta(p,\theta_\sigma,t^*,s^*)}}\right\}$$

Therefore,

$$0 \geq \min\left\{ \frac{\gamma_{p,\theta_\sigma}(s^*) - \gamma_{p,\theta_\sigma}(s)}{\beta(p,\theta_\sigma,t^*,s^*)}, \sqrt[3]{\frac{\gamma_{p,\theta_\sigma}(s^*) - \gamma_{p,\theta_\sigma}(s)}{\beta(p,\theta_\sigma,t^*,s^*)}} \right\} \tag{3.37}$$

Moreover, (1.24) and (3.32) implies $0 < t^* \leq s \leq s^* < 2$. Since $\gamma_{p,\theta_\sigma}(\cdot)$ is an increasing function on $[0,2)$, hence we have

$$\gamma_{p,\theta_\sigma}(s^*) - \gamma_{p,\theta_\sigma}(s) \geq 0 \tag{3.38}$$

But (3.37) and (3.38) implies that

$$\gamma_{p,\theta_\sigma}(s^*) - \gamma_{p,\theta_\sigma}(s) = 0 \tag{3.39}$$

because $\beta(p,\theta_\sigma,t^*,s^*) > 0$. From (3.39), we conclude that $s = s^*$ due to the monotonicity of γ_{p,θ_σ}. That is, $\lim_{j\to\infty} s_j = s$. □

4. Numerical Simulation. In this section, we will present the results of some numeical experiments. Theorem 3 and Theorem 4 serve as our guideline for the crack inspection procedure. In each step of the procedure to locate a crack, we choose the proper locaitons (referring to P and Q throughout this paper) to set the current electrodes. At the midways between two current electrodes, we measure the infinitesimal change in magnitude of the electostatic potential along the circumference (this is referring to $|\frac{\partial f_{p,q,\sigma}}{\partial \tau}|$). Recall that the midpoints on $\widehat{PQ}$ and $\widehat{QP}$ are denoted by R and N respectively. The procedure to locate a crack is stated as follows :

Procedure to locate a crack:

(1) *Arbitrarily choose P_0 and Q_0 so that they are at the end points of some diameter of the disk. Start from $P = P_0$ and $Q = Q_0$. In other words, place two current electrodes at the end points of some diameter of the disk.*

(2) *Measure $|\frac{\partial f_{p,q,\sigma}}{\partial \tau}|$ at R and N. If the measurements are identical, then there's no crack. Otherwise follow the following steps of iteration for $j = 0, 1, 2, ...$*

(3) *If the measurement at R is larger than that at N, then rotate P_j and Q_j counterclockwise along $\partial\Omega$ through an angle of $\frac{\pi}{2^{j+1}}$ to obtain P_{j+1} and Q_{j+1} respectively. If the measurement at N is larger than that at R, then rotate P_j and Q_j clockwise along $\partial\Omega$ through an angle of $\frac{\pi}{2^{j+1}}$ to obtain P_{j+1} and Q_{j+1} respectively. Go to (4).*

(4) *Set*

$$P = P_{j+1}, \qquad \text{and} \quad Q = Q_{j+1}$$

Go to (3).

(5) *As $j \to \infty$, the location of the current electrode at Q will approach the crack tip on the boundary. Terminate the process , say, at $Q = Q_j$, when the rotational angle in step (3) is sufficiently small. Let θ_σ stand for the approximate crack tip. Then take*

$$\theta_{app} = q_j.$$

To determine the crack length, the iteration in (1.23) yields a sequence of estimates which converges to the crack length provided the following information is given :

(1) An upper bound of the crack length (s_b).

(2) The exact locaiton of the exterior crack tip (θ_σ).

A natural candidate for (1) is to take s_b to be **the damage size growth limit** which is defined to be the maximum size to which initial or in-service size damage is allowed to grow without degrading the residual strength level below its required level [MS]. As for (2), if the exterior crack tip is not prominent enough to be visualizable, θ_σ can be replaced in (1.23) by θ_{app} which is obtained from the preceding procedure. We revise the computational algorithm for length determination as follows :

Procedure to size a crack:

(1) *Choose P and Q (the locations of current electrodes) so that $0 < p - \theta_\sigma < \pi/2$ (or $0 < p - \theta_{app} < \pi/2$).*

(2) *Measure* $|\frac{\partial f_{p,q,\sigma}}{\partial \tau}|$ *at the midways between* P *and* Q *(referring to* M *and* M_σ *as before), and take the ratio of these two measurements to evaluate* $\gamma_{p,\theta_\sigma}(s)$ *(recall the definition from (1.4)). This is the only data obtained from two Dirichlet boundary measurements. So the iteration functions defined in (1.21) and (1.22) actually can be expressed in terms of the boundary measurements as follows :*

$$\lambda_{\sigma,p}(\theta,y) = 2\sqrt{\frac{data-1}{\alpha(p,\theta,y)}}\Big/\left(1+\sqrt{\frac{data-1}{\alpha(p,\theta,y)}}\right),$$

and

$$\omega_{\sigma,p}(\theta,x,y) = \begin{cases} \max\left\{\min\left\{y-\frac{\gamma_{p,\theta}(y)-data}{\beta(p,\theta,x,y)}, y-\frac{\gamma_{p,\theta}(y)-data}{\beta(p,\theta,\tilde{x},y)}\right\}, \right. \\ \qquad \left. \min\left\{y-1, y-\sqrt[3]{\frac{\gamma_{p,\theta}(y)-data}{\beta(p,\theta,x,y)}}\right\}\right\}, \\ \qquad \textit{if} \quad data \geq \gamma_{p,\theta}\big(\omega^2_{\sigma,p}(\theta,x,y)\big) \ \textit{or} \ \omega^2_{\sigma,p}(\theta,x,y) < 0\ , \\ \max\left\{y-\frac{A_{p,\theta}(y)}{\phi_1(\theta,x,y)}, y-\frac{B_{p,\theta}(y)}{\phi_2(\theta,x,y)}, y-\frac{C_{p,\theta}(y)}{\phi_3(\theta,x,y)}\right\}, \\ \qquad \textit{otherwise,} \end{cases}$$

where "data" is the measurement of $\gamma_{p,\theta_\sigma}(s)$*, and* $\gamma_{p,\theta}(y)$ *is to be calculated using the formula (2.23), i.e.,*

$$\gamma_{p,\theta}(y) := \left|\frac{\tan\left(\frac{m-\theta}{2}\right)\sec^2\left(\frac{m-\theta}{2}\right)}{\tan\left(\frac{m_\sigma-\theta}{2}\right)\sec^2\left(\frac{m_\sigma-\theta}{2}\right)}\right| \cdot \left|\frac{K_y(m_\sigma-\theta)}{K_y(m-\theta)}\right| \cdot \left|\frac{[K_y(m_\sigma-\theta)+K_y(p-\theta)][K_y(m_\sigma-\theta)-K_y(q-\theta)]}{[K_y(m-\theta)-K_y(p-\theta)][K_y(m-\theta)+K_y(q-\theta)]}\right|.$$

The functions $A_{p,\theta}$*,* $B_{p,\theta}$*,* $C_{p,\theta}$*, and* ϕ_j *(*$j=1,2,3$*) are computable using the formula (1.6) - (1.8) and (1.17).* α *and* β *are explicitly defined in (1.14) and (1.18), hence they are also computable by plugging argument values for* (p,θ,x,y) *into the formula (1.6) - (1.12) and (1.17).*

(3) **Iteration Steps** *:*

$$\begin{aligned} &\textit{Set} \quad \theta^* &&= \theta_\sigma \quad (\textit{or } \theta_{app}), \\ &\qquad\ s_0 &&= s_b, \\ &\qquad\ t_0 &&= \lambda_{\sigma,p}(\theta^*, s_0). \\ &\textit{For} \quad j = 0,1,2,3,..., \\ &\qquad\ s_{j+1} &&= \omega_{\sigma,p}(\theta^*, t_j, s_j), \\ &\qquad\ t_{j+1} &&= \lambda_{\sigma,p}(\theta^*, s_{j+1}). \end{aligned}$$

(4) *When* $\theta^* = \theta_{app}$*, (1.24) and (1.25) are not necessarily true. We will consider the algorithm stable in the sense that we can still obtain an increasing sequence* t_j *and a decreasing sequence* s_j*, so that*

$$s_j \to s^* \quad as \quad j \to \infty$$

for some s^* near s whenever θ_{app} is close to θ_σ. We apply the following strategy to determine when to terminate the iteration stated in (3) :

> *Stop performing the iteration when $|s_j - s_{j-1}|$ is within the required tolerance for some j, or when*
> $$\gamma_{p,\theta_{app}}(s_j) < \underbrace{\gamma_{p,\theta_\sigma}(s)}_{\text{data}} < \gamma_{p,\theta_{app}}(s_{j-1}).$$

Recall that $\gamma_{p,\theta_\sigma}(s)$ is directly measurable from two Dirichlet boundary measurements.

(5) *Let s_{app} be the approximate length of the crack. Then take*

$$s_{app} = s_j.$$

Example. Suppose a linear crack of length 0.4 (out of 2) is located at 15° counterclockwise away from the horizontal diameter. We demonstrate in Table 1 the computational data needed for crack tip detection. Each row contains indispensable measurements at each step of iteration. "msr at R" ("msr at N") stands for $|\frac{\partial f_{p,q,\sigma}}{\partial \tau}|$ measured at R (or measured at N, respectively). We list rotation angle of P and Q to be carried out in the 4th column, where positive values indicate counterclockwise rotation and negative indicate clockwise rotation.

Crack tip Inspection Data

step, j	P	Q	rot angle	msr at R	msr at N
0	45.	225.	90	2.14042	1.6222
1	135.	315.	45.	2.07451	1.35354
2	180.	0.	22.5	2.24045	1.60883
3	202.5	22.5	11.25	1.57224	2.33525
4	191.25	11.25	5.625	2.40161	1.54612
5	196.875	16.875	2.8125	1.53114	2.44096
6	194.063	14.0625	1.40625	2.46238	1.52318
7	195.469	15.4687	0.703125	1.51909	2.47356
8	194.766	14.7656	0.351562	2.47928	1.51702
9	195.117	15.1172	0.175781	1.51598	2.48216
10	194.941	14.9414	0.0878906	2.48361	1.51545
11	195.029	15.0293	0.0439453	1.51519	2.48434
12	194.985	14.9854	0.0219727	2.48471	1.51506
13	195.007	15.0073	0.0109863	1.51499	2.48489
14	194.996	14.9963	0.00549316	2.48498	1.51496
15	195.002	15.0018	0.00274658	1.51495	2.48503

+ indicates counterclockwise rotation.

- indicates clockwise rotation.

$\theta_\sigma = 15°$, $s = 0.4$, and $\theta_{app} = q_{15} = 15.0018°$.

TABLE 1

We choose to start with P at 45° counterclockwise away from the horizontal diameter and Q at 225° counterclockwise away from the horizontal diameter ($j = 0$). It turns out $|\frac{\partial f_{p,q,\sigma}}{\partial \tau}|$ at R is larger than that at N (Table 1). According to the algorithm, at next step $j = 1$, we have to simultaneously rotate P and Q counterclockwise by 90°, where the current electrodes are therefore placed at

135° and 315° counterclockwise away from the horizontal diameter. Once again, $|\frac{\partial f_{p,q,\sigma}}{\partial \tau}|$ measured at R is greater than that measured at N. Then we rotate the electrodes counterclockwise by 45° to obtain the new locations for P and Q. Keep following the procedure in this manner – at each step, rotate the electrodes by 1/2 of the rotational amount applied at the previous step. At $j = 15$, Q is switched to the point 15.0018° counterclockwise away from the horizontal diameter (Table 1), where is considered to be close to the exact crack tip on the boundary. A graphical demonstration of this approximation procedure for the first 6 steps is displayed in Figure 4. To determine the crack length, we assume the crack growth limit is $s_b = 0.8$, and we choose P to be at $(1, 45^o)$ in the polar coordinates. That is, $p - \theta_\sigma = 30^o$. There is a reason for this particular choice of the locaitons of the current electrodes. We will discuss this issue later. In Table 2, we list the progressive data of a lower-bound sequence and an upper-bound sequence. The upper-bound sequence is used to approximate the crack length. The 4th column contains the realtive error of each approximation at different iteration steps. After 10 steps of iteration, the crack length is approximated by $s_{10} = 0.400001$.

Crack Length Inspection Data

j	s_j	t_j	error(%)
0	0.8	0.0901924	100.
1	0.625534	0.154974	56.3836
2	0.555927	0.181214	38.9817
3	0.488639	0.20484	22.1599
4	0.43729	0.22119	9.32244
5	0.410623	0.229022	2.65585
6	0.402174	0.231405	0.54355
7	0.400385	0.231903	0.0963738
8	0.400065	0.231992	0.0163248
9	0.40001	0.232008	0.00254455
10	0.400001	0.23201	0.000189227

$p - \theta_\sigma = 30^o$. $s_b = 0.8$. $s = 0.4$.
The approximate crack length is :
$s_{app} = s_{10} = 0.400001$.

TABLE 2

We have tested our algorithms on many other examples. The crack length we have simulated ranges from 0.001 to 0.4 (out of the unit disk). Recall that in our detection procedure the current electrodes at P and Q are always to be placed on the opposite sides of a diameter. Suppose we consider the detectability of an edge crack only in the sense that we are able to distinguish a damaged disk from the flawless one by two boundary measurements. Without choosing the current electrodes in a particular orientation (i.e., $p - \theta_\sigma$ could be arbitrary), we are able to detect a crack of length 0.0016 by comparing two measurements of $|\frac{\partial f}{\partial \tau}|$ at the midways between the current electrodes (immediate application of the Claim (2) preceding Theorem 2). Similar to [KSV], this requires 4 to 5 significant digits of voltage readings. In other words, using this $2D$ method, we are able to determine

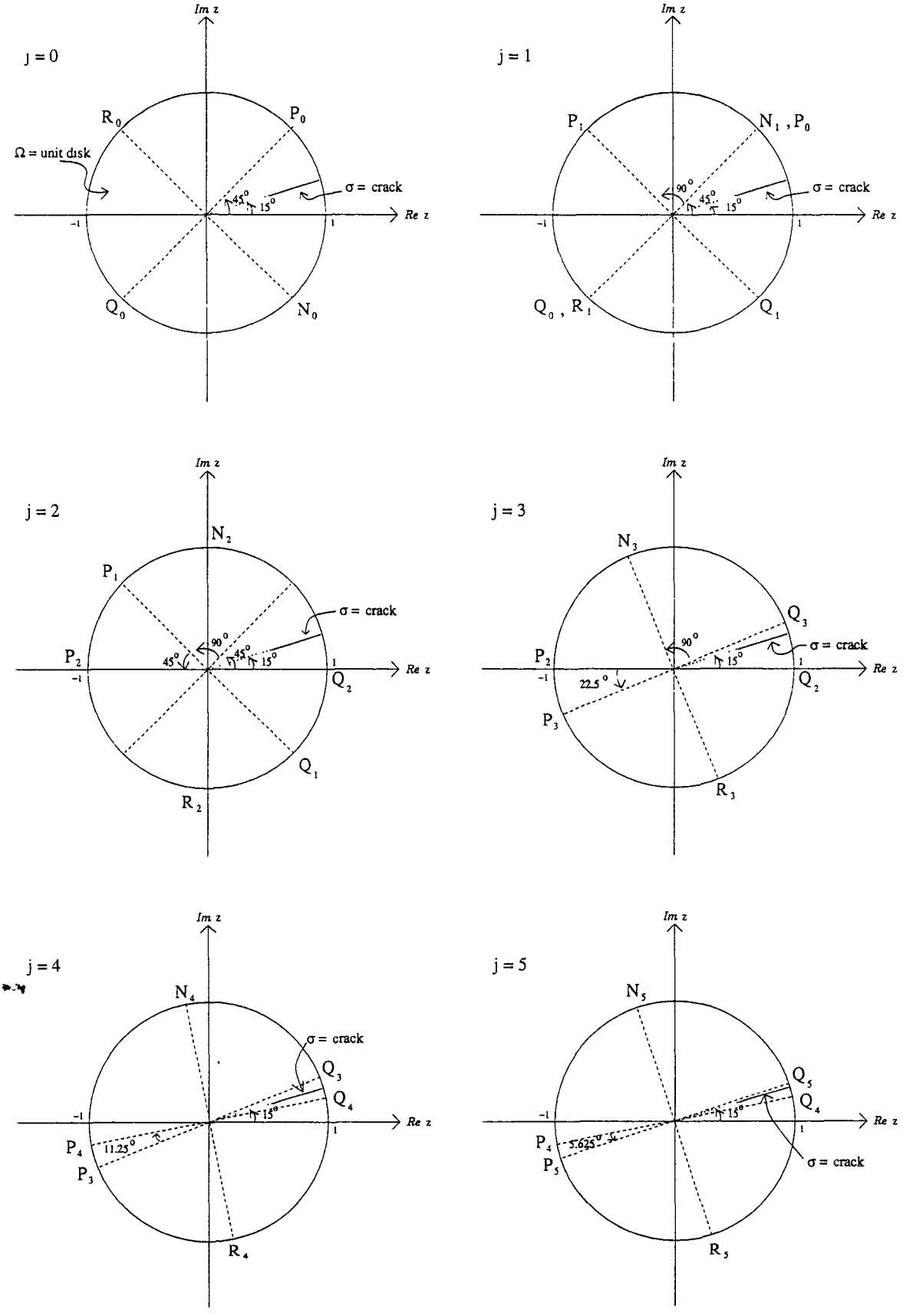

FIGURE 4. Crack length = 0.4. The surface crack tip is located at $(1, 15°)$ in polar coordinates.

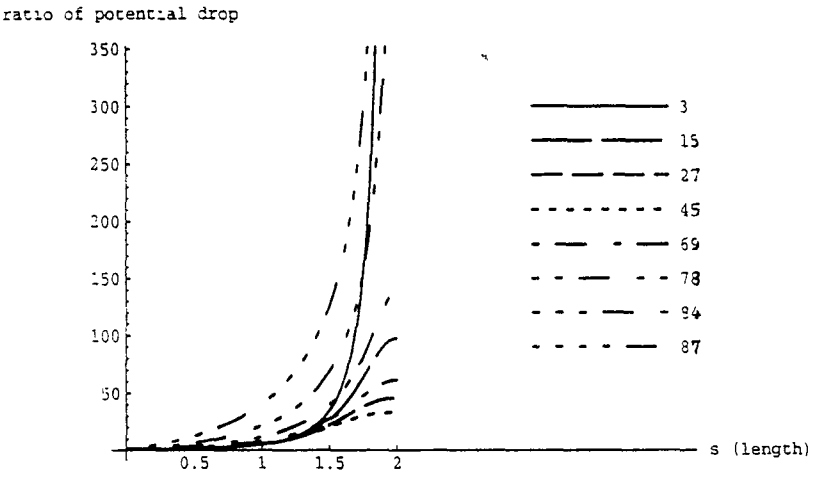

FIGURE 5. The graph of $\gamma_{p,\theta_\sigma}(s)$ associated with different values of $p-\theta_\sigma$. The number appended to the curve indicates the associated value of $p-\theta_\sigma$ measured in degrees.

whether a radial crack plane of depth ≥ 0.0016 is imbedded in a unit circular cylinder. In theorem 2, the function γ_{p,θ_σ} is characterized as an increasing function of crack length. Since γ_{p,θ_σ} is also measurable by taking the ratio of $|\frac{\partial f}{\partial \tau}|$ (which in practice represents the electrical potential difference within small distance) at the midpoints between the current electrodes, its increasing rate with crack length can be used to determine the sensitivity of the conventional potential drop method [reference]. The sensitivity depends on $p-\theta_\sigma$, the orientation of the input diameter (see Figure 1 in Section 1) relative to the detected crack plane. In Figure 5 - 10, we ploted the curves of γ_{p,θ_σ} vs. crack length at different values of $p-\theta_\sigma$ varying from 0^o and 90^o. Figure 5 shows an overview over all the possible range of crack length. Figure 6 - 10 give a closer look at different levels of crack length. We observe that for different crack lengths, γ_{p,θ_σ} changes most dramatically when $p-\theta_\sigma$ is close to 90^o. In particular when the crack length is so small as 0.0016 compared with the dimension of the domain, the variation of $\gamma_{p,\theta_\sigma}(s)$ with s becomes less prominent when the orientation of the current electrodes changes from $p-\theta_\sigma \approx 90^o$ to $p-\theta_\sigma \approx 30^o$, and then increases the effect when $p-\theta_\sigma$ decreases from 30^o to 0^o or so. The classical potential drop technique utilizes the difference of the electrostatic potential drop between a damaged specimen and a flawless specimen to estimate the size of a crack (Figure 11 - 12). For this conventional technique, the above observations can be used to identify the most sensitive locations of the current electrodes and the probing detector. In our model, a small neighborhood around 90^o away from the crack is considered to be the most sensitive area to impose the current electrode P. And the regoin between 30^o and 45^0 with respect to the crack plane is considered to be the least sensitive area to impose the current electrodes. This conclusion is independent of crack length.

The classical potential drop technique [Ha] does not provide a way to locate

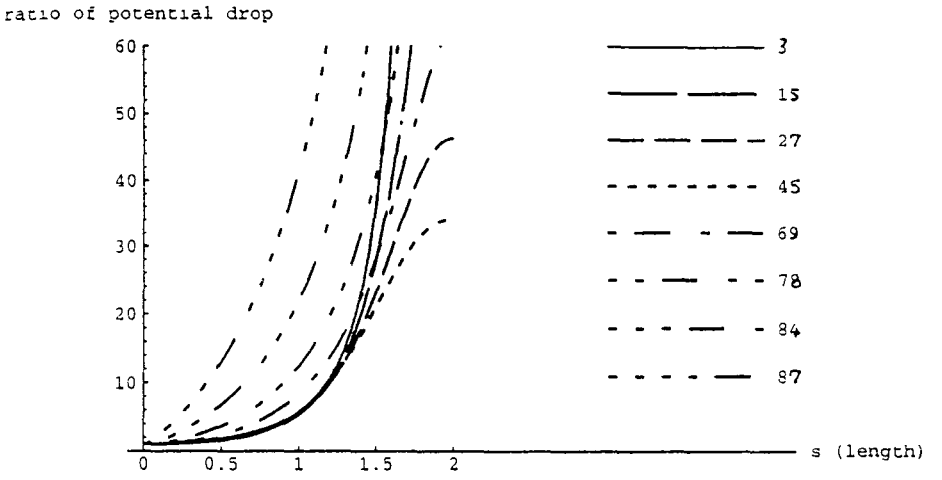

FIGURE 6. A closer look at Figure 5

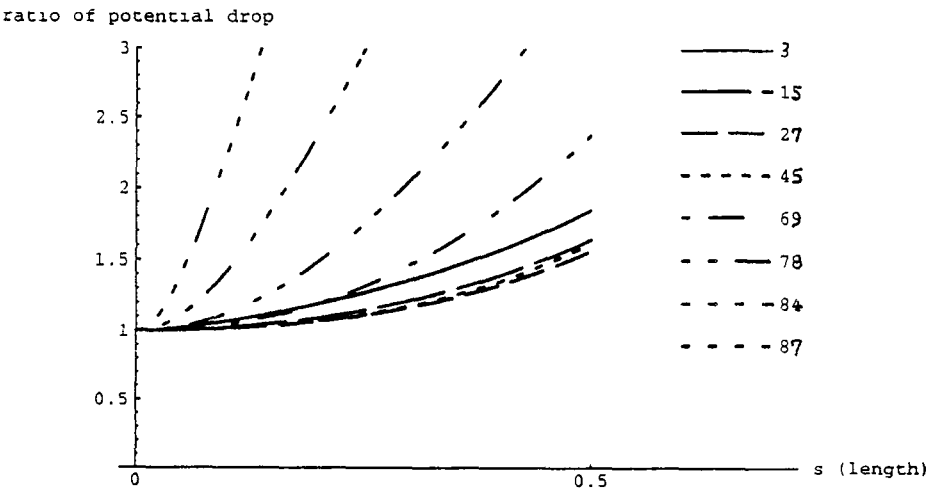

FIGURE 7. The graph of $\gamma_{p,\theta_\sigma}(s)$ associated with different values of $p - \theta_\sigma$ for s varying from 0 to 0.5. The number appended to the curve indicates the associated value of $p - \theta_\sigma$ measured in degrees.

a crack. Our inspection procedure enables us to identify the location of a radial through crack even the crack is invisible from the surface. Sensitivity is again an important issue in this detection algorithm. To be short, we switch the current electrodes on the boundary according to the difference between the potential drop at the corresponding midpoints. Suppose the current electrodes are switched to some locations where the voltage reading at two midpoints does not make any difference, then we cannot determine the appropriate locations of the current electrodes for the following steps. The drawback of this location identification procedure is that it requires certain sensitivity at "all" steps of the measurements. Nevertheless, we

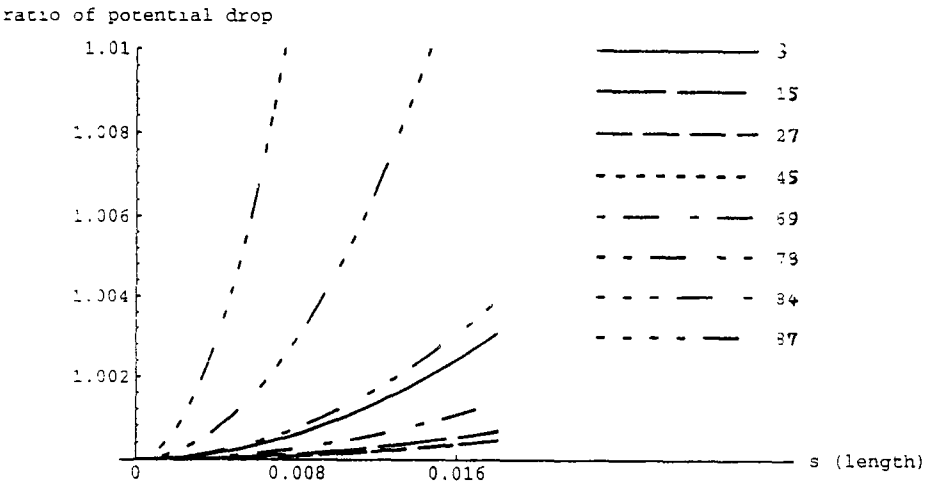

FIGURE 8. The graph of $\gamma_{p,\theta_\sigma}(s)$ associated with different values of $p - \theta_\sigma$ for s varying from 0 to 0.016. The number appended to the curve indicates the associated value of $p - \theta_\sigma$ measured in degrees.

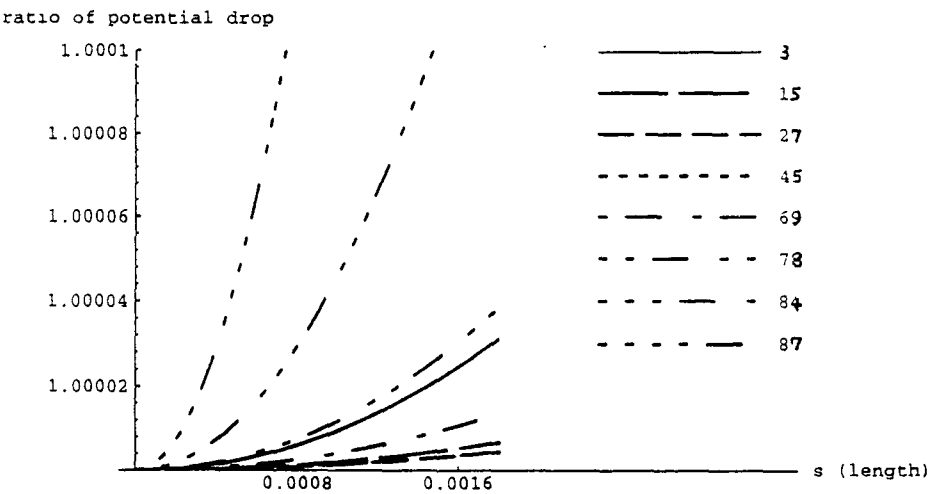

FIGURE 9. The graph of $\gamma_{p,\theta_\sigma}(s)$ associated with different values of $p - \theta_\sigma$ for s varying from 0 to 0.0016. The number appended to the curve indicates the associated value of $p - \theta_\sigma$ measured in degrees.

are still able to approximately locate a very small crack of length 0.0016 (Table 3) within a high accuracy. Though as mentioned in the previous paragraph, this requires accurate voltage readings to the 5th decimal point. From Table 1, Table 3, and many other simulation examples, we observe that it always takes 15 steps to trap the probed crack within a small region, namely, the sector bounded between Q_{14} and Q_{15}. Basically, this iteration procedure is based on a bisection technique - starting from a rotation angle of 90°, each time we rotate the current electrodes

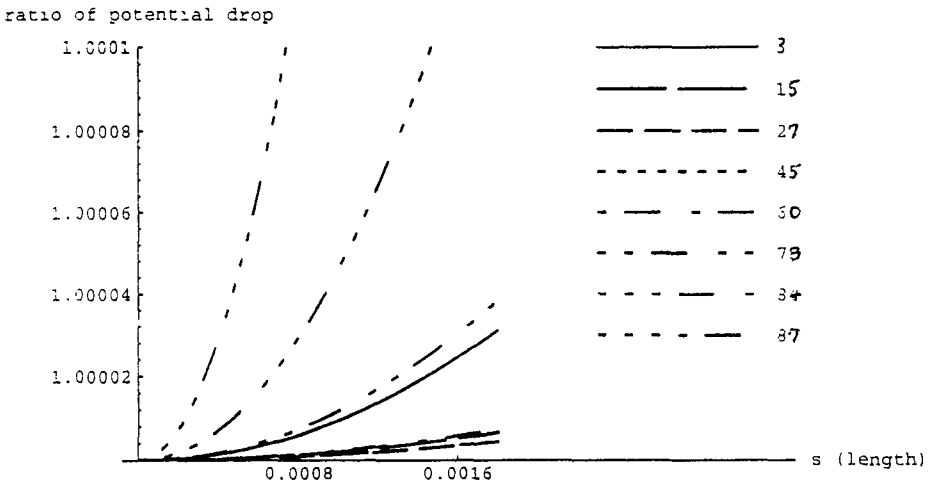

FIGURE 10. The graph of $\gamma_{p,\theta_\sigma}(s)$ associated with different values of $p-\theta_\sigma$ for s varying from 0 to 0.0016. When $30^o \leq p-\theta_\sigma \leq 60^o$, The curve increases with s slowly.

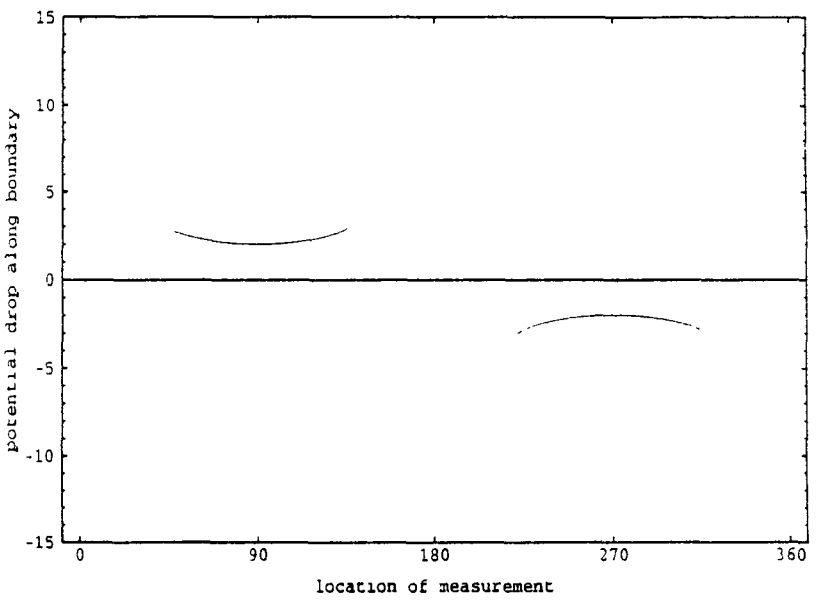

FIGURE 11. Plot of the potential drop on the boundary of a flawless disk.

by 1/2 rotational amount applied at the previous step. Hence the convergent rate significally depends on the dimension of the probed area. But at least after a finite steps of inspection, the searching region can be narrowed down to a neighborhood of the damaged area. The accuracy and convergent rate of this location trapping algorithm does not depend on crack length as long as the probed crack is detectable as we defined before for all different locations of the current electrodes.

It is a more subtle issue to find a simple relation between the effectiveness of the length algorithm and the orientation of the current electrodes with respect to the

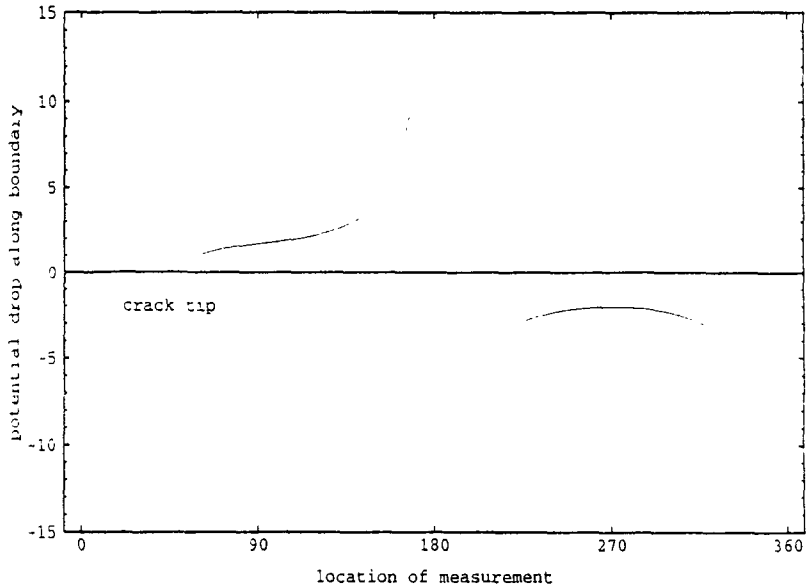

FIGURE 12. Plot of the potential drop on the boundary of a damaged disk.

Crack tip Inspection Data

#step, j	P	Q	rot angle	msr at R	msr at N
0	75.	255.	90	2.	1.99999
1	165.	345.	45.	2.	1.99999
2	210.	30.	22.5	1.99999	2.
3	187.5	7.5	11.25	2.00001	1.99999
4	198.75	18.75	5.625	1.99998	2.00002
5	193.125	13.125	2.8125	2.00004	1.99996
6	195.938	15.9375	1.40625	1.99992	2.00008
7	194.531	14.5312	0.703125	2.00015	1.99984
8	195.234	15.2344	0.351562	1.9997	2.0003
9	194.883	14.8828	0.175781	2.00055	1.99945
10	195.059	15.0586	0.0878906	1.99912	2.00088
11	194.971	14.9707	0.0439453	2.00117	1.99883
12	195.015	15.0146	0.0219727	1.99863	2.00137
13	194.993	14.9927	0.0109863	2.00148	1.99852
14	195.004	15.0037	0.00549316	1.99846	2.00154
15	194.998	14.9982	0.00274658	2.00157	1.99843

+ indicates counterclockwise rotation.

- indicates clockwise rotation.

$\theta_\sigma = 15^o$, $s = 0.0016$, and $\theta_{app} = q_{15} = 14.9982^o$.

TABLE 3

probed crack. There are two factors which affects the efficiency of the algorithm for length determination : one is the assumed upper bound s_b, and the other is the orientation of the electrode pair with respect to the probed crack. It is not surprising that the algorithm converges faster if s_b is closer to the actual length s. This can be easily explained from the formula (1.19) and (1.20) associated with the iteration function $\omega_{\sigma,p}$ since s_b is used as the initial guess in the iterations. For example, consider the case of the minimum detectable length, $s = 0.0016$. Table 4 - 11 lists the inspection data corresponding to $s_b = 0.01$, $s_b = 0.1$, $s_b == 0.8$, and $s_b = 1.2$ respectively. We present the results simulated with two different orientations of the current electrodes : $p - \theta_\sigma = 30^o$ and $p - \theta_\sigma = 45^o$. We observe that in both cases, the number of iterations required for a certain accuracy (say,

Crack Length Inspection Data

j	s_j	t_j	error(%)
0	0.01	0.00112872	525.
1	0.00515186	0.00113015	221.991
2	0.00282957	0.00113082	76.8478
3	0.00186795	0.00113109	16.7471
4	0.00161926	0.00113117	1.20347
5	0.0016001	0.00113117	0.00626369
6	0.00159999	0.00113117	0.000921697

$p - \theta_\sigma = 30°$. $s_b = 0.01$. $s = 0.0016$.

The approximate crack length is :

$s_{app} = s_{10} = 0.00159999$.

TABLE 4

Crack Length Inspection Data

j	s_j	t_j	error(%)
0	0.01	0.00112876	525.
1	0.0051515	0.00113018	221.969
2	0.00282937	0.00113085	76.8355
3	0.0018679	0.00113112	16.744
4	0.00161928	0.00113119	1.20516
5	0.00160014	0.0011312	0.00876997
6	0.00160003	0.0011312	0.00159673
7	0.00160003	0.0011312	0.00159648
8	0.00160003	0.0011312	0.00159647
9	0.00160003	0.0011312	0.00159647

$p - \theta_\sigma = 45°$. $s_b = 0.01$. $s = 0.0016$.

The approximate crack length is :

$s_{app} = s_9 = 0.00160003$.

TABLE 5

with the error less than 0.01%) increases with s_b. This phenomenon is global in the sense that it is true with different orientations of the current electrodes. We also observe that even though we use an approximate crack tip as the input data (i.e., $\theta^* = \theta_{app}$), the length algorithm works effectively in all the examples under the condition $30^0 \leq p - \theta_\sigma \leq 60^0$ and $0.0016 < s_b < 1.2$. It all takes less than 20 steps of iterations to converge to an estimate within 0.05% of the relative error. However, under the same condition $30^0 \leq p - \theta_\sigma \leq 60^0$, it takes about 40 iteration steps to achieve the same accuracy as s_b increases to 1.5. If we increase s_b to 1.8, then the approximating sequence $\{s_j\}$ stays far beyond 0.0016 even after 100 steps of iterations. Whenever we use an approximate crack tip $\theta^* = \theta_{app}$, we have to worry about the stability which has been defined in step (4) of the algorithm. For all the tested examples of different crack lengths (varying from 0.0016 to 0.4), the condition $30^0 \leq p - \theta_\sigma \leq 60^0$ yields a stable length algorithm under a reasonable assumed upper bound. This stability condition is minimal within the detectability of our method. That is, if the crack length is larger than 0.0016, then the condition $30^0 \leq p - \theta_\sigma \leq 60^0$ can be relaxed to a larger range in order to obtain a stable length algorithm.

To explore the effect of $p - \theta_\sigma$ on the length algorithm, we further perform the

Crack Length Inspection Data

j	s_j	t_j	error(%)
0	0.1	0.00109535	6150.
1	0.0531399	0.00111444	3221.24
2	0.0273901	0.00112332	1611.88
3	0.0139398	0.00112754	771.239
4	0.00711014	0.00112958	344.384
5	0.0037463	0.00113056	134.144
6	0.00221697	0.00113099	38.5609
7	0.00168607	0.00113115	5.37968
8	0.00160219	0.00113117	0.136788
9	0.00159999	0.00113117	0.000826841

$p - \theta_\sigma = 30^o$. $s_b = 0.1$. $s = 0.0016$.

The approximate crack length is :

$s_{app} = s_{11} = 0.00159999$.

TABLE 6

Crack Length Inspection Data

j	s_j	t_j	error(%)
0	0.1	0.00109578	6150.
1	0.0527513	0.00111472	3196.95
2	0.0271273	0.00112346	1595.46
3	0.0137974	0.00112762	762.337
4	0.00703786	0.00112963	339.866
5	0.00371164	0.0011306	131.977
6	0.00220277	0.00113103	37.6734
7	0.00168271	0.00113118	5.16965
8	0.00160206	0.0011312	0.128885
9	0.00160003	0.0011312	0.00167753
10	0.00160003	0.0011312	0.00159648
11	0.00160003	0.0011312	0.00159647
12	0.00160003	0.0011312	0.00159647

$p - \theta_\sigma = 45^o$. $s_b = 0.1$. $s = 0.0016$.

The approximate crack length is :

$s_{app} = s_{12} = 0.00160003$.

TABLE 7

calculations for $p-\theta_\sigma \approx 0^o$ and for $p-\theta_\sigma \approx 90^o$, whcih are considered better choice concerning the sentivity of the classical ptential drop method. For $p - \theta_\sigma \approx 0^o$ when $s = 0.0016$, it takes 46 iteration loops to achieve an error within 1% by assuming $s_b = 0.01$ and using the exact crack tip $\theta^* = \theta_\sigma$. If we use an approximate value $\theta^* = \theta_\sigma$ as the input data, then it needs 54 iteration steps to bound the error within 1%. Compared with the result for $p - \theta_\sigma = 30^o$ or $p - \theta_\sigma = 45^o$ (Table 4 - 5), the algorithm yields much slower convergent rate when $p - \theta_\sigma \approx 0^o$. The algorithm does not work well and is very unstable for small cracks when the current electrodes have a 90^o orientation with respect to the probed crack. For example, consider $s = 0.0016$ and $\theta_\sigma = 15^o$. Recall that the output data is given by $\gamma_{p,\theta_\sigma}(s) = \left|\frac{\partial f_{p,q,\sigma}}{\partial \tau}(m)\right| \Big/ \left|\frac{\partial f_{p,q,\sigma}}{\partial \tau}(m_\sigma)\right|$, where $\frac{\partial f_{p,q,\sigma}}{\partial \tau}(m_\sigma)$ is measured near by the crack tip when $p - \theta_\sigma \approx 90^o$. This leads to the oscillations in the course of iterations even when we use $\theta^* = \theta_\sigma$ (Table 12). Using the approximate crack tip $\theta_{app} = 15.0049^o$ for θ^*, we obtain an estimate $s_{app} = 0.006401$ with the error

Crack Length Inspection Data

j	s_j	t_j	error(%)
0	0.8	0.000308941	49900.
1	0.628832	0.000544543	39202.
2	0.303963	0.000958205	18897.7
3	0.193	0.00104467	11962.5
4	0.110458	0.00109054	6803.6
5	0.0591402	0.00111221	3596.26
6	0.0305915	0.00112228	1811.97
7	0.015587	0.00112704	874.186
8	0.0079368	0.00112934	396.05
9	0.00414404	0.00113044	159.002
10	0.00238379	0.00113095	48.9871
11	0.00172921	0.00113113	8.0756
12	0.00160483	0.00113117	0.301618
13	0.00159999	0.00113117	0.000464141

$p - \theta_\sigma = 30°$. $s_b = 0.8$. $s = 0.0016$.

The approximate crack length is :

$s_{app} = s_{13} = 0.00159999$.

TABLE 8

Crack Length Inspection Data

j	s_j	t_j	error(%)
0	0.8	0.000320078	49900.
1	0.609081	0.000580138	37967.6
2	0.218577	0.00102911	13561.1
3	0.124044	0.0010846	7652.73
4	0.0663469	0.00110966	4046.68
5	0.0343591	0.0011211	2047.45
6	0.0175192	0.00112649	994.95
7	0.00890877	0.00112908	456.798
8	0.00461637	0.00113033	188.523
9	0.00258934	0.00113092	61.8335
10	0.00178957	0.00113115	11.848
11	0.00161009	0.0011312	0.630517
12	0.00160006	0.0011312	0.0035663
13	0.00160003	0.0011312	0.00159649
14	0.00160003	0.0011312	0.00159647
15	0.00160003	0.0011312	0.00159647

$p - \theta_\sigma = 45°$. $s_b = 0.8$. $s = 0.0016$.

The approximate crack length is :

$s_{app} = s_{15} = 0.00160003$.

TABLE 9

59.9% after 45 iteration loops under the assumption $s_b = 0.01$. What has happened here to the length algorithm seems to be in contrast to our observations as to the sensitivity associated with the classsical potential drop technique.

Summing up our observations regarding length determination, we draw the following conclusions :

(1) The orientation of the input curren electrodes (represented by the value of $p - \theta_\sigma$) is crucial in determining the stability and the effectiveness of the length algorithm. In particular when the probed crack is small, the effect of this orientation becomes more prominent.

(2) Let the locatios of the current electrodes be our boundary input. Within

Crack Length Inspection Data

j	s_j	t_j	error(%)
0	1.2	0.000039519	74900.
1	1.16619	0.0000487312	72786.8
2	1.1268	0.0000616916	70324.8
3	1.07997	0.0000807305	67398.3
4	1.02283	0.00011025	63826.9
5	0.950542	0.00015923	59308.9
6	0.854182	0.000247502	53286.4
7	0.714621	0.000420597	44563.8
8	0.479122	0.0007591	29845.1
9	0.36033	0.000902374	22420.6
10	0.241815	0.00101036	15013.4
11	0.14466	0.00107328	8941.28
12	0.0795048	0.00110419	4869.05
13	0.0416597	0.00111853	2503.73
14	0.0213366	0.00112526	1233.54
15	0.0108461	0.00112847	577.879
16	0.00556947	0.00113003	248.092
17	0.00302085	0.00113076	88.803
18	0.00193519	0.00113108	20.9493
19	0.00162909	0.00113116	1.81824
20	0.00160025	0.00113117	0.0153714
21	0.00159999	0.00113117	0.000920613

$p - \theta_\sigma = 30^\circ$. $s_b = 1.2$. $s = 0.0016$.

The approximate crack length is :

$s_{app} = s_{21} = 0.00159999$.

TABLE 10

Crack Length Inspection Data

j	s_j	t_j	error(%)
0	1.2	0.0000446876	74900.
1	1.16229	0.0000560249	72543.
2	1.11758	0.0000724336	69748.9
3	1.06324	0.0000974189	66352.4
4	0.994903	0.000138	62081.4
5	0.904696	0.000209568	56443.5
6	0.776317	0.000348958	48419.8
7	0.567694	0.000640139	35380.8
8	0.110196	0.00109117	6787.23
9	0.0584683	0.00111263	3554.27
10	0.0301548	0.00112248	1784.68
11	0.0153514	0.00112715	859.466
12	0.00781703	0.0011294	388.564
13	0.00408598	0.00113049	155.374
14	0.00235903	0.00113098	47.4396
15	0.00172247	0.00113116	7.65433
16	0.00160439	0.0011312	0.274267
17	0.00160003	0.0011312	0.00196799
18	0.00160003	0.0011312	0.00159647
19	0.00160003	0.0011312	0.00159647

$p - \theta_\sigma = 45^\circ$. $s_b = 1.2$. $s = 0.0016$.

The approximate crack length is :

$s_{app} = s_{19} = 0.00160003$.

TABLE 11

the detectability of our method (i.e., for $s \geq 0.0016$), there is a minimal stability region for the the boundary input. Given an appropriate upper bound s_b, this minimal stability region is characterized by the condition $30^\circ \leq p - \theta_\sigma \leq 60^\circ$. If the input current electrodes are imposed on this

Crack Length Inspection Data

j	s_j	t_j	error(%)
0	0.01	0.000314787	525.
1	0.00967447	0.000318308	504.655
2	0.00934547	0.000321861	484.092
3	0.00901296	0.00032544	463.31
4	0.00867691	0.000329039	442.307
5	0.00833728	0.00033265	421.08
6	0.00799406	0.000336265	399.628
7	0.00764723	0.000339875	377.952
8	0.00729679	0.000343469	356.049
9	0.00694274	0.000347035	333.922
10	0.00658512	0.000350561	311.57
11	0.00622393	0.000354031	288.996
12	0.00585923	0.000357431	266.202
13	0.00549108	0.000360744	243.192
14	0.00511955	0.000363954	219.972
15	0.00474472	0.000367041	196.545
16	0.00436671	0.000369987	172.919
17	0.00398564	0.000372772	149.103
18	0.00360166	0.000375376	125.104
19	0.00321492	0.000377781	100.933
20	0.0028256	0.000379966	76.6002
21	0.00243389	0.000381914	52.1184
22	0.00203999	0.000383607	27.4993
23	0.00164407	0.00038503	2.75449
24	0.00146895	0.000385568	8.19049
25	0.00199062	0.0003838	24.4134
26	0.000444351	0.000387556	72.228
27	0.00515603	0.000363645	222.252
28	0.00478153	0.000366745	198.845
29	0.00440382	0.000369705	175.239
30	0.00402305	0.000372507	151.441
31	0.00363934	0.00037513	127.459
32	0.00325287	0.000377555	103.304
33	0.00286379	0.000379763	78.9871
34	0.00247231	0.000381734	54.5194
35	0.00207861	0.000383453	29.9132
36	0.00168288	0.000384903	5.18024
37	0.00135368	0.000385891	15.3951

$p - \theta_\sigma = 89.994°$. $s_b = 0.01$. $s = 0.0016$.
$\theta^* = \theta_\sigma$.

TABLE 12

region, the algorithm is not only stable but also converges very fast. There is certain choice for the boundary input we would always like to avoid. Our simulation indicates a neighborhood around 90^o off the probed crack plane is considered to be the most unstable area to attach the current electrodes to.

(3) The initial upper bound s_b can not be too large in order to speed up the convergent rate of the algorithm. Nevertheless, we think the assumed upper bound is a minor factor in determning the effectiveness of the algorithm. For the minimum detectable length $s = 0.0016$, we are still able to obtain a good estimate (within 20 iteration steps) by starting with $s_b = 1.2$ if we carefully choose the input current electrodes in the minimal stability region.

Even though we have tackled a model with simple geometry, we are convinced

that the stability and the sensitivity quesitons are far more complicate to answer completely from our computational observations. However, we believe that by generalizing the ideas implemented in this paper, we can treat these problems in a more analytic way and in a more general setting [BCW].

Acknowledgments. We thank Dr. Fourney of Aerospace Engineering Department and Dr. Samford of Mechanical Engineering Department at University of Maryland for many interesting conversations. We also thank Dr. Vogelius and Dr. Santosa for providing useful information.

REFERENCE

[A] G. Alessandrini, *Stable determination of a crack from boundary measurements*, proc. Royal Soc. Edinb. Ser A **123** (1993), no. 3, 497 – 516.

[ABV] G. Alessandrini, E.Beretta, and S Vessella., *Determining linear cracks by boundary measurements – Lipschitz stability.*, SIAM J. Math. Anal. to appear.

[BCW] C. Berenstein, D. C. Chang, and E. Wang, *A stability property of surface cracks*, in progress.

[BV1] K. Bryan and M. Vogelius, *A uniqueness result concerning the identification of a collection of cracks from finitely many electrostatic boundary measurements*, SIAM J. Math. Anal. **23** (1992), no. 4, 950 – 958.

[BV2] ———, *A computational algorithm to Determine crack locations from electrostatic boundary measurements. The case of multiple cracks*, Int. J. Engng Sci. **32** (1994), no. 4, 579 – 603.

[C] J. M. Coffey, *Mathematical modeling in NDT – What it is and what it does*, The institute of mathematics and its applications conference series (M. Blakemore and G. Georgiou, eds.), Oxford, 1986.

[EH] A. R. Elcrat and C. Hu., *Determination of surface and interior cracks from electrostatic measurements using Schwarz-Christoffel transformations*, Int. J. Eng. Science to appear.

[EIN] A. R. Elcrat, V. Isakov, and O. Neculoiu, *On finding a surface crack from boundary measurements*, Inverse Problems **11** (1995), 343 – 352.

[FV] A. Friedman and M. Vogelius, *Determine cracks by boundary measurements*, Indiana Math. J. **38** (1989), 527 – 556.

[Ha] R. Halmshaw, *Nondestructive Testing*, Wiley-Interscience.

[He] P. Henrici, *Appled And Computational Complex Analysis*, vol. I, John Wiley & Sons, U.S.A..

[KS] P. G. Kaup and F. Santosa, *Nondestructive evaluation of corrosion damage using electrostatic measurements*, J. Nondestructive Evaluation to appear.

[KSV] P. G. Kaup, F. Santosa, and M. Vogelius, *A method for imaging corrosion damage in thin plates from electrostatic data*, Technical Report **CTC95TR219** (1995), Cornell Theroy Center, Ithaca.

[MS] Military Specification, *Airplane Damage Tolerance Requirements*, MIL-A-83444 (1974), USAF.

[SV] F. Santosa and M. Vogelius, *A computational algorithm to determine cracks from electrostatic boundary measurements*, Int. J. Engng Sci. **29** (1991), no. 8, 917 – 937.

APPENDIX A

A CONFORMAL MAPPING FROM $\Omega \setminus \sigma$ ONTO THE UNIT DISK $\{z \in \mathbb{C} | |z| < 1\}$ IN $\mathbb{C}$-PLANE

In this section we explicitly construct a one-to-one conformal transform which maps the crack domain $\Omega \setminus \sigma$ onto the open unit disk $\{z \in \mathbb{C} | |z| < 1\}$. The existence of an analytic map from a connected damain onto another connected domain is guaranteed by the Riemann mapping theorem. We coustruct the mapping by taking the composition of 6 intermediate one-to-one analytic functions. One cannot ignore the asymptotic behavior of the conformal map near the boundary of $\Omega \setminus \sigma$ in order to calculate the potential on the boundary. In other words, finally we need consdier a topological extension of this map to the closure of $\Omega \setminus \sigma$. Through a translation and a rotation, $\Omega \setminus \sigma$ could be placed in a position so that Ω is centered at the origin and σ lies on the real axis of the complex plane with the surface crack tip located at $z = 1$. Therefore without loss of generality, we can assume that $\Omega = \{z \in \mathbb{C} | |z| < 1\}$ and σ lies on the positive real axis. Let $a = 1 - s$. That is, assume the interior crack tip is located at $z = a$ in the complex plane.

STEP 1.

First, we map $\Omega \setminus \sigma$ onto the region defined by

$$\Omega_1 = \{z \in \mathbb{C} | \mathrm{Re} z \leq 0\} \setminus \{z \in \mathbb{C} | (a-1)/(a+1) \leq \mathrm{Re} z \leq 0, \mathrm{Im} z = 0\}$$

via the linear fractional transformation h_1 given as follows:

$$h_1(z) = \frac{z-1}{z+1}$$

STEP 2.

Rotate Ω_1 clockwise through an angle of $\pi/2$ to obtain the region

$$\Omega_2 = \{z \in \mathbb{C} | \mathrm{Im} z \geq 0\} \setminus \{z \in \mathbb{C} | \mathrm{Re} z = 0, 0 \leq \mathrm{Im} z \leq (1-a)/(1+a)\}$$

This could be done by taking an analytic function h_2 defined by

$$h_2(z) = -iz$$

STEP 3.

Set

$$h_3(z) = z^2$$

Then h_3 conformally maps Ω_2 onto the region defined by

$$\Omega_3 = \mathbb{C} \setminus \left\{ z \in \mathbb{C} | \mathrm{Im} z = 0, \mathrm{Re} z \geq -\left(\frac{1-a}{1+a}\right)^2 \right\}$$

STEP 4.

Shift Ω_3 to the right $\left(\frac{1-a}{1+a}\right)^2$ units. Equivalently, if we let

$$h_4(z) = z + \left(\frac{1-a}{1+a}\right)^2$$

then h_4 will map Ω_3 onto the following region:

$$\Omega_4 = \mathbb{C} \setminus \{z \in \mathbb{C} | \mathrm{Re} z \geq 0, \mathrm{Im} z = 0\}$$

STEP 5.

Let's define a mapping as follows:

$$h_5(z) = z^{1/2}$$

where we take the branch $\{z \in \mathbb{C} | 0 < \arg(z) < 2\pi\}$ for the square root in the complex plane so that h_5 is analytic in Ω_4. It is easy to see that the mapping h_5 maps the region Ω_4 onto the upper half plane, denoted by Ω_5.

STEP 6.

Now, the upper half plane Ω_5 can be mapped onto the unit disk $\{z \in \mathbb{C} | |z| < 1\}$ through a familiar Möbius transform. We achieve this if we define the following Möbius transform:

$$h_6(z) = \frac{i - z}{i + z}$$

then h_6 conformally maps the upper half plane onto the unit disk which is centered at the origin.

Finally, we take the composition of those conformal maps calculated form STEP 1 through SETP 6. Let us denote this conformal transform by $\tilde{h}_\sigma$, where the subscript s indicates the dependence of the map on crack length. We obtain

$$\begin{aligned} \tilde{h}_\sigma(z) &= (h_6 \circ h_5 \circ h_4 \circ h_3 \circ h_2 \circ h_1)(z) \\ &= \frac{i - \left(\left(\frac{s}{2-s}\right)^2 - \left(\frac{z-1}{z+1}\right)^2\right)^{1/2}}{i + \left(\left(\frac{s}{2-s}\right)^2 - \left(\frac{z-1}{z+1}\right)^2\right)^{1/2}} \end{aligned} \tag{A.1}$$

Again, we would like to emphasize that we consider the branch $\{z \in \mathbb{C} | 0 < \arg(z) < 2\pi\}$ whenever the square root is involved in the calculations.

$\tilde{h}_\sigma$ is a one-to-one analytic function from $\Omega \setminus \sigma$ onto $\{z \in \mathbb{C} | |z| < 1\}$, hence the inverse exists in the interior of $\Omega \setminus \sigma$. However, this is not sufficient for solving the boundary value problem (0.1) since $\tilde{h}_\sigma$ is not continuous over the entire closure of $\Omega \setminus \sigma$. Actually, as we carefully examine the preceding calculations, we observe that

in step 3, $h_3(z) = z^2$ maps the negative real axis onto the positive real axis. Due to the branch taken in step 5, $h_5(z) = z^{1/2}$ will not send back the positive real axis into the negaive real axis again. So the entire boundary of $\Omega \setminus \sigma$ is in reality mapped onto the upper half circle only. As the consequence, $\tilde{h}_\sigma$ will be discontinuous when a sequence of points approach the crack edge and the lower half boundary from the interior of the lower half plane. Fortunately, this drawback can be remedied by implementing "Osgood-Carathéodory theorem". We state the theorem as follows and refer readers to [He] for further reference:

Definition. A region is called a **Jordan region** if it is the interior of a Jordan curve.

Definition. A map of one set onto another is called **topological** if it is one-to-one and continuous in both direction.

Theorem ("Osgood-Carathéodory theorem"). *let D and D^* be two Jordan regions. Any function mapping D conformally and one-to-one onto D^* can be extended to a topological map of the closure of D onto the closure of D^*.*

Although $\Omega \setminus \sigma$ is not a Jordan region, we could divide it into two Jordan regions by a simple arc whose one end is at the interior crack tip and the other end could be any point of $\partial\Omega$ other than the surface crack tip. Applying Osgood-Carathéodory theorem to these two Jordan subregions, it is possible to topologically extend $\tilde{h}_\sigma$ to the entire closure of $\Omega \setminus \sigma$. In practice, We proceed in the following way. Let's denote by $\mathbb{R}^2_+$ the upper half plane and $\mathbb{R}^2_-$ the lower half plane. Define

$$\begin{aligned} &\Omega^+ = \Omega \cap \mathbb{R}^2_+ \\ &\Omega^- = \Omega \cap \mathbb{R}^2_- \\ &\partial\Omega^+ = \partial\Omega \cap \mathbb{R}^2_+, \qquad \text{and} \qquad \partial\Omega^- = \partial\Omega \cap \mathbb{R}^2_- \end{aligned} \tag{A.2}$$

Regarding σ as a double-edged slit, the upper edge is denoted by σ^+ and the lower part by σ^-. That is, we have $\sigma = \sigma^+ \cup \sigma^-$. Define $h_\sigma : \overline{\Omega \setminus \sigma} \to \overline{\Omega}$ by

$$h_\sigma(z) := \begin{cases} \tilde{h}_\sigma(z), & \text{for} \quad z \in \Omega \setminus \sigma \\ \lim\limits_{\Omega^+ \ni z_n \to z} \tilde{h}_\sigma(z_n), & \text{for} \quad z \in \partial\Omega^+ \cup \sigma^+ \\ \lim\limits_{\Omega^- \ni z_n \to z} \tilde{h}_\sigma(z_n), & \text{for} \quad z \in \partial\Omega^- \cup \sigma^- \end{cases} \tag{A.3}$$

Then h_σ is the topological map of $\tilde{h}_\sigma$ extended to the closure of $\Omega \setminus \sigma$. The inverse of h_σ exists in the sense that it is analytic from Ω onto $\Omega \setminus \sigma$, continuous and one-to-one from $\overline{\Omega}$ onto $\overline{\Omega \setminus \sigma}$.